Geological Survey of Canada

CURRENT RESEARCH
2007-C1

Detrital zircon geochronology of the Archean volcano-sedimentary sequence of the Barclay belt and the Paleoproterozoic marble-quartzite sequence of the Northern Chantrey group, Boothia mainland area, Kitikmeot region, Nunavut

A.M. Hinchey, J.J. Ryan, W.J. Davis, L. Nadeau, and D.T. James

2007

CURRENT RESEARCH

Natural Resources Canada
Ressources naturelles Canada

Canada

ISSN 1701-4387
Catalogue No. M44-2007/C1E-PDF
ISBN 978-0-662-45916-3

A copy of this publication is also available for reference in depository libraries across Canada through access to the Depository Services Program's Web site at http://dsp-psd.pwgsc.gc.ca

A free digital download of this publication is available from GeoPub: http://geopub.nrcan.gc.ca/index_e.php

Toll-free (Canada and U.S.A.): 1-888-252-4301

Critical reviewer
N. Wodicka

Authors

A.M. Hinchey (alanahinchey@gov.nl.ca)
Geological Survey
Department of Natural Resources,
Government of Newfoundland
and Labrador
P.O. Box 8700,
St. John's, Newfoundland
A1B 4J6

W.J. Davis (bidavis@nrcan.gc.ca)
Geological Survey of Canada
601 Booth Street
Ottawa, Ontario K1A 0E8

J.J. Ryan (jryan@nrcan.gc.ca)
Geological Survey of Canada,
625 Robson Street,
Vancouver, British Columbia
V6B 5J3

L. Nadeau (LNadeau@nrcan.gc.ca)
Geological Survey of Canada,
490 rue de la Couronne,
Québec, Quebec G1K 9A9

D.T. James (djames@nrcan.gc.ca)
Canada-Nunavut Geoscience Office
626 Tumiit Plaza,
Iqaluit, Nunavut X0A 0H0

Publication approved by GSC Central

Correction date:

Detrital zircon geochronology of the Archean volcano-sedimentary sequence of the Barclay belt and the Paleoproterozoic marble-quartzite sequence of the Northern Chantrey group, Boothia mainland area, Kitikmeot region, Nunavut

A.M. Hinchey, J.J. Ryan, W.J. Davis, L. Nadeau, and D.T. James

Hinchey, A.M., Ryan, J.J., Davis, W.J., Nadeau, L., and James, D.T., 2007: Detrital zircon geochronology of the Archean volcano-sedimentary sequence of the Barclay belt and the Paleoproterozoic marble-quartzite sequence of the Northern Chantrey group, Boothia mainland area, Kitikmeot region, Nunavut; Geological Survey of Canada, Current Research 2007-C1, 19 p.

Abstract: The 'Boothia mainland area', in the Kitikmeot region of Nunavut, is located in the northern Rae Domain of the western Churchill Province. The area is characterized by variable deformed and metamorphosed volcano-sedimentary rocks of the Barclay belt; metaplutonic rocks, which dominate the region; and a marble-quartzite sequence that is informally referred to as the Northern Chantrey group. Detrital zircon geochronology studies of three samples were conducted using the Sensitive High-Resolution Ion Micro Probe to constrain the timing of deposition of the supracrustal sequences in the mapping area. A sample of psammitic schist from the volcano-sedimentary Barclay belt gave a maximum depositional age of 2764 ± 23 Ma based on the youngest detrital zircon. Two samples of psammitic schist from different stratigraphic levels within the Northern Chantrey group gave a maximum depositional age of 2454 ± 13 Ma based on the youngest detrital zircon age.

Résumé : La « terre continentale de Boothia », dans la région de Kitikmeot du Nunavut, se situe dans la partie nord du domaine de Rae de la Province de Churchill occidentale. Ce secteur est caractérisé par la présence d'unités déformées et métamorphisées à des degrés divers qui se composent de roches volcanosédimentaires de la ceinture de Barclay, de roches métaplutoniques, qui forment la lithologie prédominante de la région, et d'une séquence de marbre-quartzite attribuée de manière informelle au groupe de Northern Chantrey. Des analyses géochronologiques de zircons détritiques de trois échantillons ont été effectuées à la microsonde ionique à haute résolution et à haut niveau de sensibilité (SHRIMP) afin d'encadrer dans le temps le dépôt des séquences supracrustales dans la région cartographique. Un échantillon de schiste psammitique de la ceinture volcanosédimentaire de Barclay a fourni un âge de dépôt maximal de 2 764 ± 23 Ma d'après l'âge sur zircon détritique le plus récent. Deux échantillons de schiste psammitique provenant de niveaux stratigraphiques différents dans le groupe de Northern Chantrey ont fourni un âge de dépôt maximal de 2 454 ± 13 Ma d'après l'âge sur zircon détritique le plus récent.

INTRODUCTION

The Boothia mainland area (informal name, Fig. 1) in the Kitikmeot region of central Nunavut is the focus of a multiyear geoscience mapping program, jointly funded by the Geological Survey of Canada and Canada-Nunavut Geoscience Office. Fieldwork initiated in 2005 was focused primarily on bedrock mapping (1:250 000 scale) of NTS map areas 57 A and 57 B, with reconnaissance mapping extended to map areas 57 C and 57 D to the north. In addition, detailed local surficial mapping and regional ice-flow studies supported a regional update of the Quaternary geology of Boothia mainland area (Tremblay, 2005). Prior to the 2005 field season, an aeromagnetic survey (Coyle et al., 2005a, b, c, d, e, f, g, h, i, j, k, l, m, n, o, p, q, r, s, t, u, v) and a remote predictive map for the region were produced, which enabled a more strategic approach to bedrock mapping.

The area is underlain chiefly by Archean granitoid metaplutonic rocks and derived gneissic rocks. It includes two isolated and lithologically contrasting supracrustal belts tentatively correlated on the basis of field relationships and lithological affinities with the Neoarchean volcano-sedimentary Barclay belt and the Paleoproterozoic Chantrey Group comprising a quartzite-marble-pelite sequence (J.J. Ryan, L. Nadeau, A.M. Hinchey, D.T. James, H.A. Sandeman, R.G. Berman, W.J. Davis, and M.D. Young, unpub. manuscript, 2007).

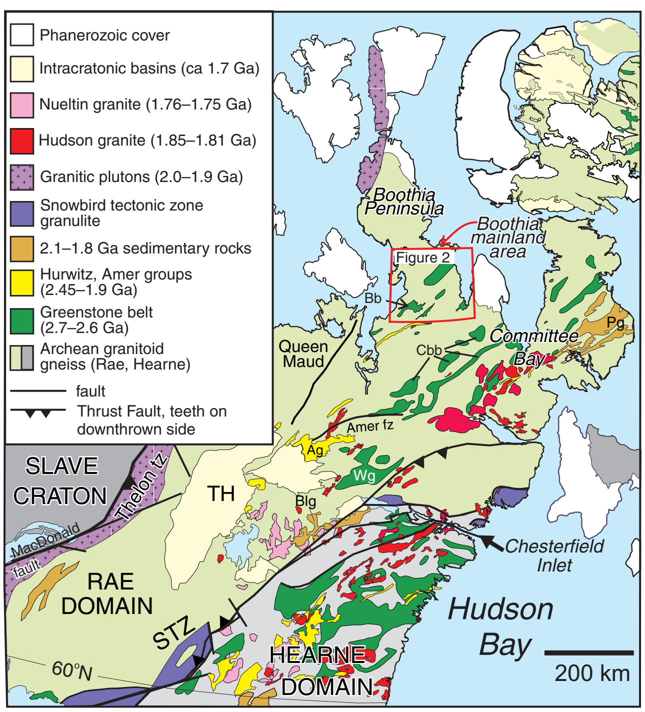

Figure 1. General geology of parts of the western Churchill Province and environs (*modified from* Berman et al., 2005). Abbreviations: Ag: Amer Group, Amer fz: Amer fault zone, Blg: Baker Lake Group, Bb: Barclay belt, Cbb: Committee Bay belt, Pg: Penhryn Group, STZ: Snowbird tectonic zone, TH: Thelon formation, tz: tectonic zone, Wg: Woodburn Lake group. The Boothia mainland map area and Figure 2 are outlined in red.

This report presents the detrital zircon U-Pb SHRIMP data obtained from three samples representative of these two belts of supracrustal rocks with the aim: to constrain their maximum depositional age, and to evaluate the stratigraphic parentage of these supracrustal successions with other comparable belts of the Rae Domain. It includes the first detrital zircon analysis for any Chantrey Group rocks.

REGIONAL GEOLOGICAL SETTING

The western Churchill Province comprises two fundamental Archean crustal divisions termed the Rae and Hearne domains (Fig. 1), and is also characterized by Paleoproterozoic successor sedimentation, magmatism, and tectonothermal reworking (Hoffman, 1988). The Boothia mainland area occurs within the Rae Domain, which is bound by the 2.0–1.9 Ga Thelon-Taltson orogen to the northwest and is separated from the Hearne Domain by the geophysically defined Snowbird tectonic zone to the southeast (Gibb and Walcott, 1971; Hoffman, 1988, 1990; Berman et al., 2005, and references therein). The Rae Domain comprises attenuated, dominantly lower-greenschist- to amphibolite-facies metamorphosed, 3.05–2.63 Ga supracrustal belts that were intruded by voluminous ca. 2.6 Ga granitoid rocks and were variably reworked during at least two Paleoproterozoic tectonothermal events (Fig. 1; Skulski et al. (2003) and references therein; Berman et al. (2005)).

Major Neoarchean supracrustal belts in the eastern Rae Domain include the Woodburn Lake group, Prince Albert Group, Mary River Group, and the Barclay belt. These belts comprise intercalated komatiitic flows, iron-formation, quartzite, pelite, and felsic tuff units, and are interpreted to have continental affinities (Heywood, 1961; Jackson, 2000; Zaleski et al., 2001; Skulski et al., 2003; Bethune and Scammell, 2003).

Voluminous and widespread 2640–2580 Ma I-type granitoid intrusions occur throughout the Rae Domain (LeCheminant and Roddick, 1991; Zaleski et al., 2001; Skulski et al., 2003). These plutons intruded the Archean supracrustal belts and range in composition from diorite to granite (*sensu stricto*; Skulski et al. (2003) and references therein). These metaluminous intrusions are spatially associated with minor peraluminous intrusions comprising two-mica and garnet-biotite granitic rocks. The peraluminous intrusions are interpreted as being contemporaneous with the metaluminous intrusions (Sandeman et al., 2005). Some of the metaluminous granitic plutons contain Nd isotopic signatures and inherited zircon cores that indicate interaction with older Mesoarchean basement, whereas some other rocks preserve more juvenile Nd isotopic signatures (Sandeman et al., 2005; T. Skulski, unpub.

data, 2006). Protoliths for rocks in the current study area are interpreted to be mainly composed of ca. 2.6 Ga metaluminous granitoid rocks.

Paleoproterozoic metasedimentary rocks occur throughout the Rae Domain (Fig. 1). These include: the dominantly quartzite, carbonate, sulphidic mudstone of the less than 1.95 Ga and more than 1.85 Ga Amer Group (Patterson, 1986; Tella, 1994; R.H. Rainbird, W.J. Davis, and S.J. Pehrsson, talk presented at Western Churchill Metallogeny Project Spring 2004 Meeting, Ottawa, Ontario, April 29–30, 2004; Geological Survey of Canada; (http://ess.nrcan.gc.ca/2002_2006/nrd/wchurchill/project_8_2_pres_21_e.php [accessed February 15, 2006]); W.J. Davis and R.H. Rainbird, unpub. data, 2006); the lower clastic and carbonate sequence and upper carbonaceous shale and/or arkosic wacke of the ca. 1.88 Ga Penrhyn Group (Henderson, 1983); siliciclastic, carbonate, and mafic volcanic sequence of the less than 2.16 Ga and more than 1.90 Ga Piling Group (Scott et al., 2002 and references therein; N. Wodicka, talk presented at Western Churchill Metallogeny Project Spring 2004 Meeting, Ottawa, Ontario, April 29–30, 2004); quartzite, marble, pelite sequence of the Chantrey Group (Frisch, 2000); and the arkose-carbonate sequence of Folster Lake Group (Frisch, 1982; Skulski et al., 2003). Generally these Paleoproterozoic sedimentary sequences preserve two phases of deformation, and are typically only metamorphosed to greenschist facies, though they can locally preserve amphibolite- to granulite-facies rocks.

Paleoproterozoic plutons of regional importance within the Rae Domain include: 2.4–2.0 Ga plutonic rocks of the western Rae Domain (*see* Berman et al. (2005) for summary); the 2.0–1.93 Ga calc-alkaline suite and younger orogenic granitoid rocks of the Thelon tectonic zone (Fig. 1) and Taltson magmatic zone (Bostock and van Breemen, 1994; McNicoll et al. 2000; McDonough et al., 2000); and ca. 1.85–1.81 Ga Hudson granites abundant in the northeastern Rae Domain (e.g. Peterson et al., 2002, and references therein). Northwest-trending Mesoproterozoic Mackenzie diabase dykes cut Archean and Paleoproterozoic units in the Rae Domain.

GEOLOGICAL OVERVIEW OF THE BOOTHIA MAINLAND AREA

The Boothia mainland area comprises variably reworked Archean continental crust containing minor amounts of Archean and Paleoproterozoic (meta)sedimentary cover preserved in two distant belts outcropping in the southwest and north-central parts of the study area (Fig. 2).

Granitoid terrain

The area is dominated by voluminous granitoid plutons that generally experienced upper-amphibolite facies metamorphism. Metamorphic grade tends to increase in the northeast direction across the study area from middle amphiblite facies in the southwest to granulite facies defining a broad zone in the northeast part of the region (Fig. 2). The metaplutonic rocks are generally characterized by biotite±hornblende±magnetite monzogranite, as well as volumetrically minor intrusions ranging from diorite to syenogranite. In the granulite belt to the northeast, the metaplutonic rocks are orthopyroxene bearing. Porphyritic (augen) monzongranite to granodiorite occur as mappable intrusions throughout the area. The state of strain also varies across the region; the metaplutonic vary from massive to weakly deformed in the southwest to highly strained and strongly gneissic in the eastern and northern parts of the study area.

Barclay belt

Archean supracrustal rocks, termed the Barclay belt (Frisch, 2000, and references therein), form narrow, northeast-striking, dismembered belts consisting of volcanic and sedimentary rocks that outcrop discontinuously from the southeast shore of Chantrey Inlet into the Boothia mainland area (Fig. 2). The belts consist mainly of psammite, semipelite, metabasalt, local ultramafic horizons, and sulphide-bearing (lean) iron-formation (Fig. 3). On the basis of similarity of lithological units, these rocks have been interpreted as equivalents to the Prince Albert Group (Frisch, 2000). Until now, however, no age data were available for volcanic sedimentary components of the Barclay belt to confirm such stratigraphic parentage. The metaplutonic rocks and derived gneissic rocks that dominate the region (Fig. 2) are interpreted to have intruded this package of supracrustal rocks. In the southwestern portion of the map area, the supracrustal rocks preserve upper-greenschist-facies to lower-amphibolite-facies metamorphic conditions. A sample from a psammitic schist from the lower part of the stratigraphic column was selected for detrital zircon geochronological analysis. Figure 3 highlights the position of the geochronology sample in the simplified stratigraphic column.

Northern Chantrey group

The second supracrustal sequence in the Boothia mainland area is dominated by marble, pelitic schist with minor psammitic schist, and quartzite layers (Fig. 4). This succession is preserved in fold keels in the central map area and unconformably overlies the foliated monzogranite intrusions that dominate the region (Fig. 4 *see* Kraft (2006) for details). The sedimentary package was metamorphosed to at least upper-amphibolite-facies conditions and the pelitic units contain garnet-sillimanite-cordierite-bearing leucosome. The correlation with the Chantrey Group is based on lithological affinities and the absence of intrusive relationships with Neoarchean intrusive bodies. This belt is referred to herein as the Northern Chantrey group. Two samples from psammitic layers at different stratigraphic levels were selected for detrital

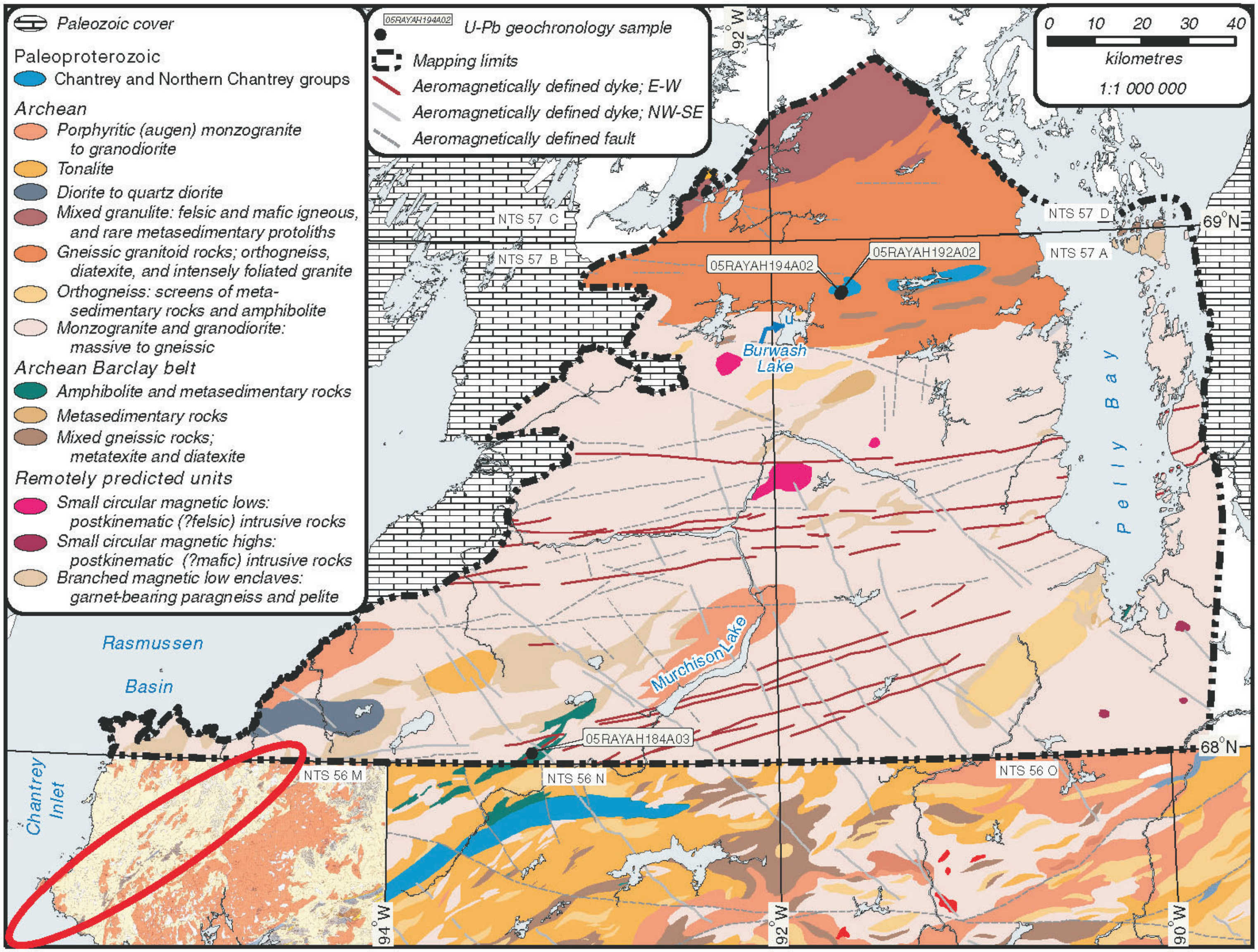

Figure 2. Simplified geology and remotely predicted geology of the Boothia mainland area. The red outline in the southwest corner of the map area outlines the type section of the Barclay belt, grey unit on the map, described in Frisch (2000). Geochronological samples referred to in the text are identified. The legend defines the geological features north of 68°N. Geological units shown south of 68°N and east of 94°W are those of Sandeman et al. (2005) and the scanned map south of 68°N and west of 94°W is that of Frisch (1982). In general, the unit colours defined for the geology north of 68°N conforms to the units of Sandeman et al. (2005), although Sandeman et al. (2005) is subdivided in more detail than in the legend.

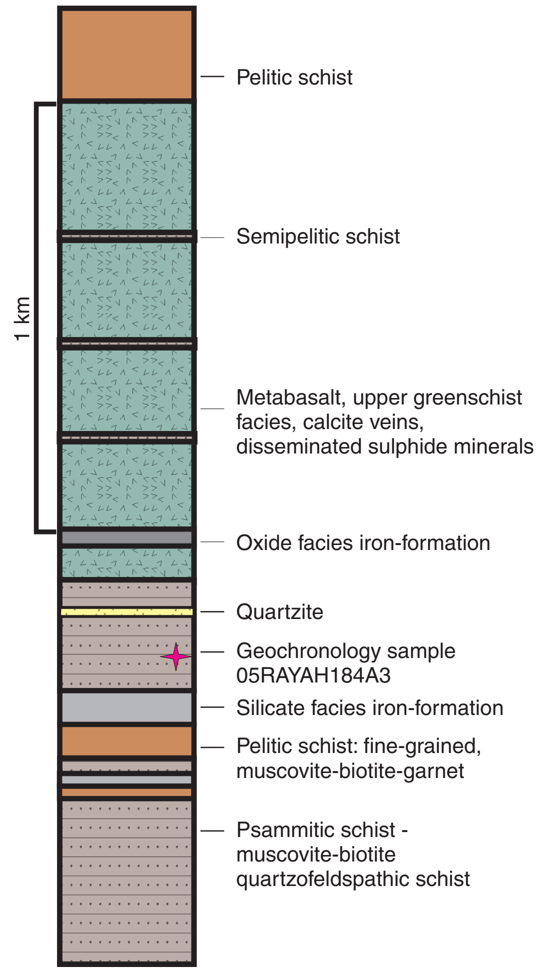

Figure 3. Schematic stratigraphic section of the volcano-sedimentary sequence of the Barclay belt showing the inferred stratigraphic position of the U-Pb geochronology sample 05RAYAH184A3; Ms = muscovite, Bt = biotite, Grt = garnet.

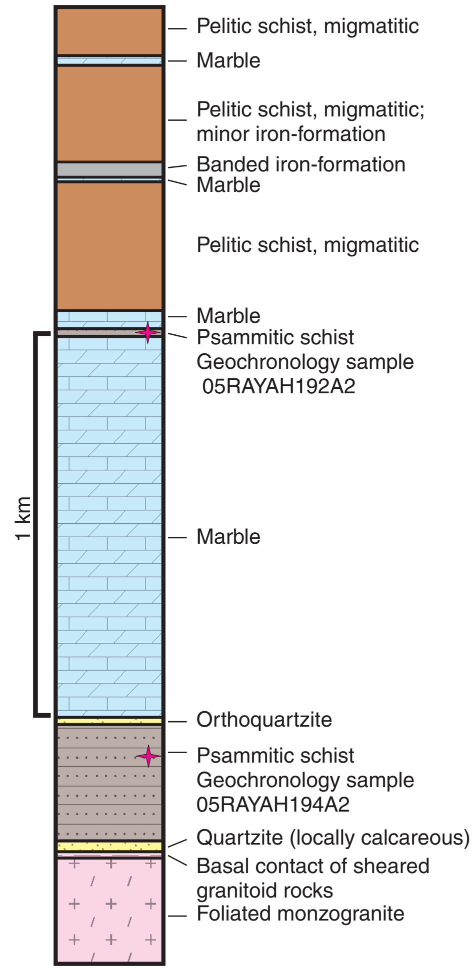

Figure 4. Schematic stratigraphic section of the marble-quartzite sequence of the Northern Chantrey group showing the inferred stratigraphic position of the U-Pb geochronology samples 05RAYAH192A2 and 05RAYAH194A2.

zircon geochronological analysis. One sample is from a psammitic schist just above the basal contact with a sheared monzogranite and the second sample is from a psammitic layer within a thick section of marble, higher in the sequence. Figure 4 highlights the position of the geochronology samples in the simplified stratigraphic column.

Crosscutting diabase dykes

All map units are crosscut by at least two undeformed dyke sets. Northwest-trending dykes are inferred to be part of the 1267 Ma Mackenzie dyke swarm (LeCheminant and Heaman, 1989). The other set is an east- and east-northeast-striking swarm that has not been previously reported in the area. The age of this swarm is presently unknown; however, they are cut by the northwest-trending dyke swarm provisionally associated with the Mackenzie swarm.

SAMPLES AND PETROGRAPHIC DESCRIPTIONS

Sample 05RAYAH184A3 (laboratory sample number z8799) is a muscovite-biotite psammitic schist from the lower section of the volcano-sedimentary sequence of the Barclay belt exposed in the southwestern portion of the map area (NTS 57 B), west of Murchison Lake (Fig. 2, 3). In outcrop, the psammitic schist (Fig. 5a) is interlayered at the centimetre- to decimetre-scale with garnet-muscovite-biotite semipelitic schist, and locally contains layers of silicate facies iron-formation. It was not possible to ascertain, from field characteristics alone, whether this schist is derived from a volcanic or a sedimentary parentage; however, in thin section, rounded eyes of quartz and feldspar, wrapped by aligned muscovite and biotite, are best interpreted as detrital grains (Fig. 5b). In addition, the strongly layered nature of the rock, its interlayered relationship with quartzite, pelite, and banded iron-formation, and the detrital grain signature (*see* below) support its interpretation as having a sedimentary rather than volcanic protolith.

Sample 05RAYAH192A2 (laboratory sample number z8801) consists of sillimanite-biotite psammitic schist from relatively higher in the marble-quartzite sequence of the Northern Chantrey group exposed in the north-central map area (NTS 57 A), northeast of Burwash Lake (Fig. 2, 4). In outcrop, the unit is a medium-grained biotite-rich psammitic schist interlayered with calcareous-quartzite at the scale of 50 cm (Fig. 6a). In hand sample, the foliation wraps porphyroblasts of coarse, recrystallized plagioclase. In thin section, biotite defines the foliation, minor sillimanite occurs as fibrolite, and perthitic intergrowths of plagioclase and potassium feldspar are preserved (Fig. 6b).

Sample 05RAYAH194A2 (laboratory sample number z8802; Fig. 2, 4) is a sillimanite-biotite psammitic schist collected from near the basal contact of the Northern Chantrey group with foliated monzogranitic basement. In outcrop, the unit is a medium-grained schist that is cut by a folded and boudinaged pegmatite vein. The sample is well foliated and fine grained. In thin section, biotite and sillimanite define the foliation, and some sillimanite grains are pseudomorphed by muscovite (Fig. 6c).

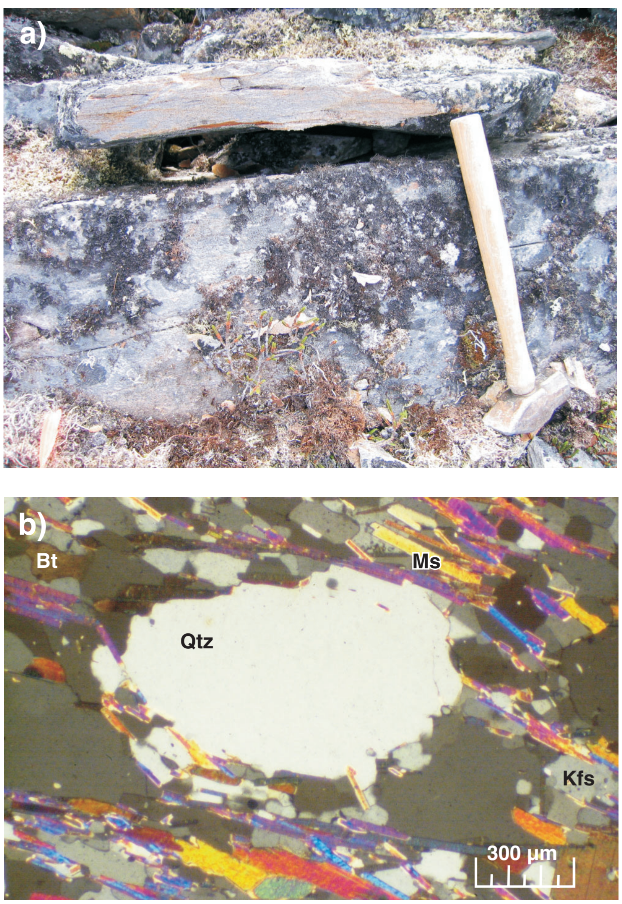

Figure 5. A sample of a muscovite-biotite psammitic schist from the Barclay belt (05RAYAH184A3). **a)** Photograph of the psammitic schist in outcrop, hammer for scale is 40 cm; and **b)** photomicrograph of the psammitic schist depicting the rounded quartz grains and foliation defined by muscovite and biotite; Bt = biotite, Ms = muscovite, Kfs = K-feldspar, Qtz = quartz.

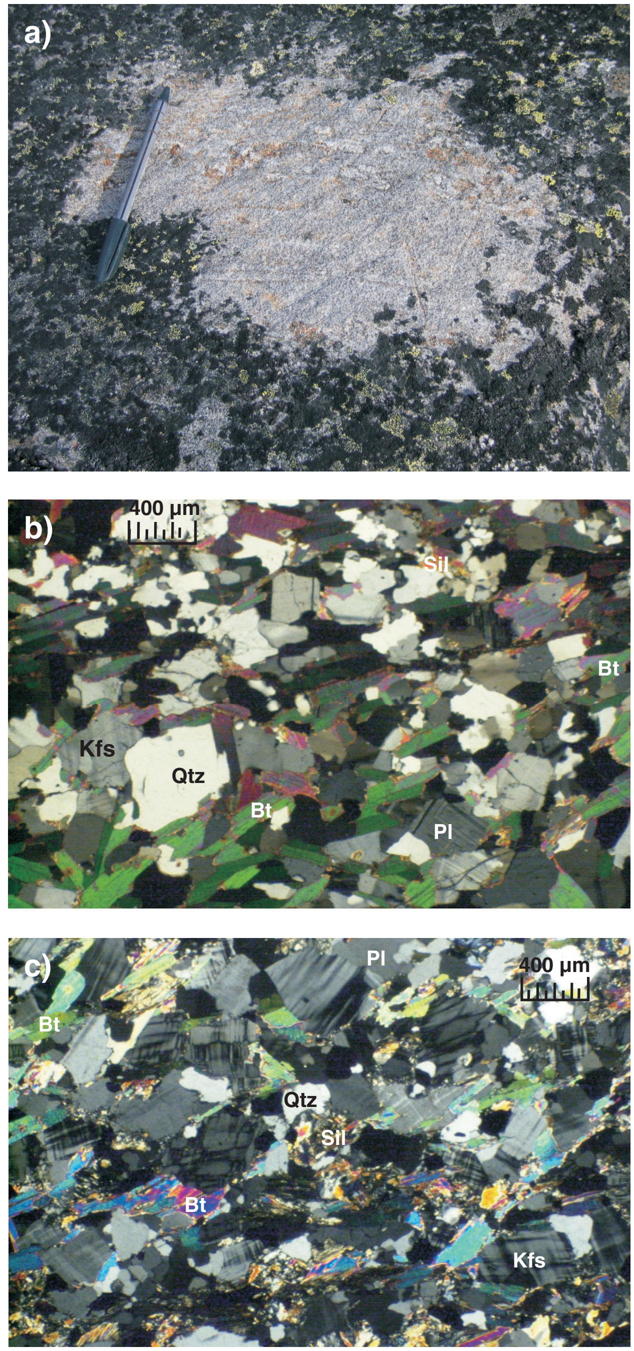

Figure 6. A sample of the sillimanite-biotite psammitic schist (05RAYAH192A2) from the Northern Chantrey group in outcrop **a)** with the black areas representing lichen (pen for scale is 15 cm) and **b)** in a photomicrograph highlighting the foliation defined by sillimanite and biotite. **c)** Photomicrograph of the sillimanite-biotite psammitic schist sample 05RAYAH194A2 from the basal unit of the Northern Chantrey group; Sil = sillimanite, Bt = biotite, Kfs = K-feldspar, Qtz = quartz, Pl = plagioclase.

ANALYTICAL PROCEDURE

Samples collected weighed up to 2 kg and the geographic sample locations are illustrated in Figure 2. Ion microprobe analysis of zircon was performed using the SHRIMP II at the Geological Survey of Canada, following the procedure described by Stern (1997), with standards and U-Pb calibration methods following Stern and Amelin (2003). Zircon grains were cast in 2.5 cm diameter epoxy mounts (GSC #IP283) along with fragments of the GSC laboratory standard zircon (z6266), which has a $^{206}Pb/^{238}U$ date of 559 Ma. Internal sections of the grains were exposed by grinding and polishing using 9 µm, 6 µm, and 1 µm diamond compound. The internal features of the zircon grains (such as zoning, internal domains, and alteration) were characterized using backscattered-electron (BSE) imaging utilizing a Cambridge Instruments scanning electron microscope. Grain-mount surfaces were evaporatively coated with 10 nm Au of high purity. The SHRIMP analyses were conducted using an $^{16}O^-$ primary beam, projected onto the zircons at 10 kV. The sputtered area used for analysis was about 35 µm in diameter with a beam current of about 13 nA. For the zircon analyses, the count rates of ten isotopes of Zr^+, U^+, Th^+, and Pb^+ were sequentially measured over five scans with a single electron multiplier and a pulse-counting system that has a deadtime of 35 ns. Off-line data processing was accomplished using customized in-house software. A 1σ external error for $^{206}Pb/^{238}U$ ratios reported in the data tables incorporate a ±1.0% error in calibrating the standard zircon (*see* Stern and Amelin, 2003). No fractionation correction was applied to the Pb-isotope data. The common Pb correction utilized the measured $^{204}Pb/^{206}Pb$ ratios and compositions modelled after Cumming and Richards (1975). Isoplot v. 3.00 (Ludwig, 2003) was used to calculate weighted means of the dates.

RESULTS

Sample 05RAYAH184A3, muscovite-biotite psammitic schist (Barclay belt)

In plane-light microscopy, zircon grains are colourless to medium brown, with many grains appearing clear to slightly turbid (Fig. 7a). The zircon population is dominated by prismatic, subhedral, colourless to light brown zircon (*see* grain 12 in Fig. 7), and contains minor elongate, subhedral, clear to turbid grains, which can display fractured ends. Backscattered-electron (BSE) imaging of grains revealed oscillatory zoning in most grains; however, some appear homogeneous (Fig. 7b).

Sixty-seven analyses were conducted on 57 different zircon grains. The results are plotted on a concordia diagram (Fig. 8a) and a cumulative probability curve (Fig. 8b). Ages range from 3774 Ma to 2764 Ma. The majority of data are less than 5% discordant (Appendix A). The most prominent age modes are 2850 Ma (n ≅ 7), 2925 Ma (n ≅ 6), 3000 Ma (n ≅ 7), and 3210 Ma (n ≅ 4). The youngest grains identified were grains 31 and 44 in Appendix A. Multiple analysis of the youngest grain, 44, yielded a weighted mean $^{207}Pb/^{206}Pb$ age of 2764 ± 23 Ma (2σ error, n = 5; MSWD = 0.2; probability of fit = 94%; Ludwig (2003)). This result is the maximum age estimate of deposition of this unit within the Barclay belt.

Sample 05RAYAH192A2, sillimanite-biotite psammitic schist (Northern Chantrey group, upper marker unit)

The quantity of zircon recovered from this sample was low, totalling only 21 grains. In plane-light microscopy, zircon grains are generally light to dark brown and turbid in appearance (Fig. 9a). The zircon population is dominated by

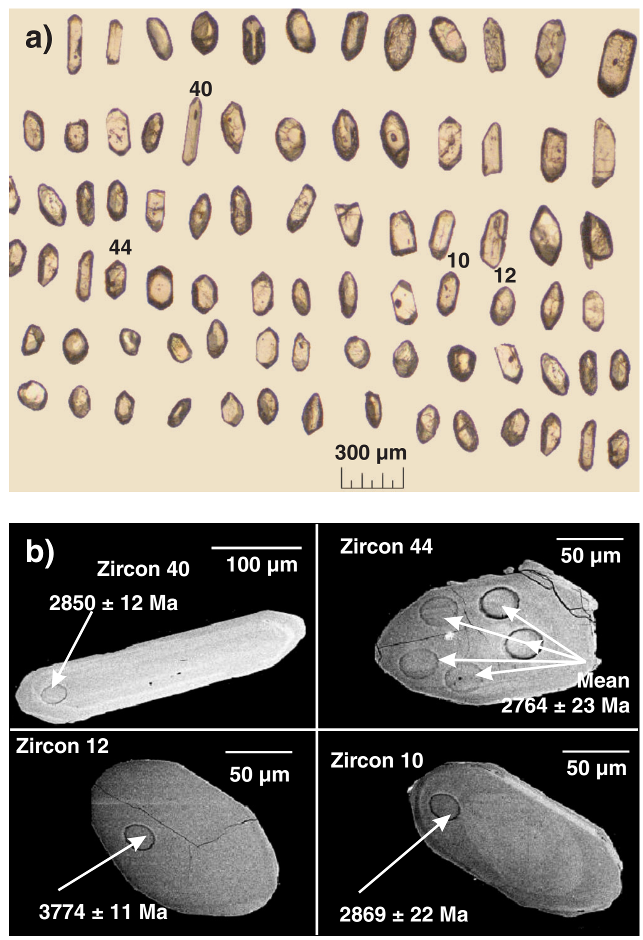

Figure 7. a) Transmitted-light image of detrital zircon grains picked from sample 05RAYAH184A3, a muscovite-biotite psammitic schist from the Barclay belt. Numbers in figure refer to the grain-identification numbers used during SHRIMP analysis and referred to in the text and in Appendix A. **b)** Backscattered-electron images of a representative selection of zircon grains. The internal zoning of the zircon grains and the pit left by the ion beam appear in the images. The $^{207}Pb/^{206}Pb$ dates are reported by the analytical site (*see* Appendix A for details). Zircon numbers correspond to spot numbers listed in Appendix A.

equant, rounded grains and fractured pieces (*see* grain 8 in Fig. 9a). In BSE images, grains generally exhibit patchy zoning or weak oscillatory zoning, and reveal their highly fractured nature (Fig. 9b).

Thirteen grains were analyzed and the results are plotted on a concordia diagram (Fig. 10a) and a cumulative probability curve (Fig. 10b). Ages range from 2915 Ma to 2505 Ma. Most data are less than 5% discordant (Appendix A). The most prominent age mode is 2560 Ma (n ≅ 6). The youngest grain yielded a $^{207}Pb/^{206}Pb$ age of 2505 ± 18 Ma (2σ error; single determination) and is interpreted as the maximum depositional age for this unit.

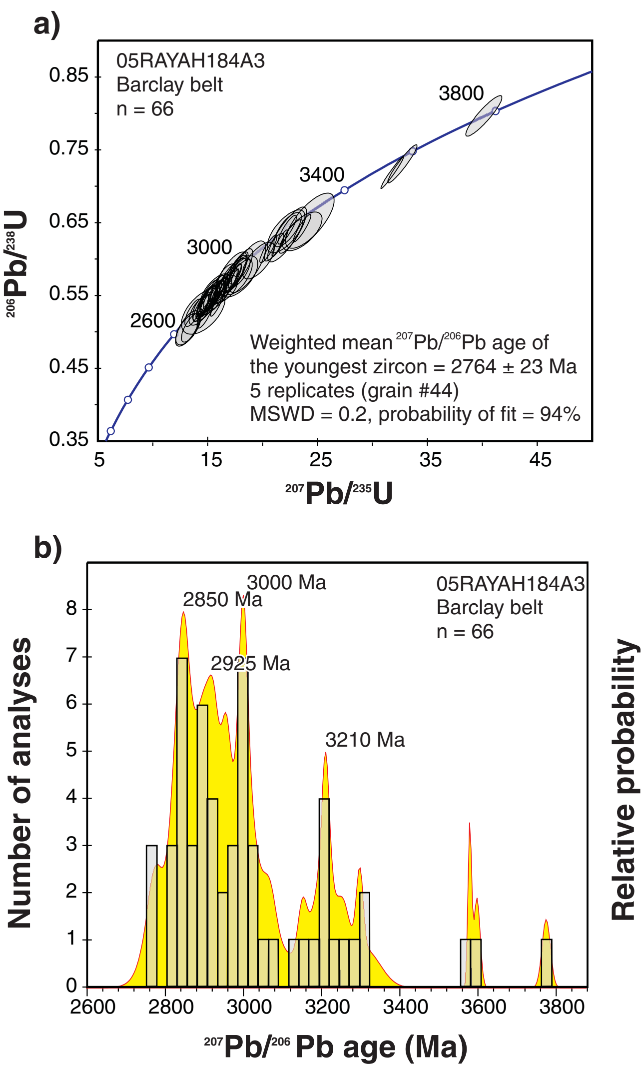

Figure 8. a) Concordia diagram of U-Pb results from sample 05RAYAH184A3, a muscovite-biotite psammitic schist from the Barclay belt. Error ellipses are at 2σ level. **b)** Cumulative probability curve where the curve represents a weighted cell-less summed probability histogram, into which errors of individual analysis have been incorporated. Grey columns represent a frequency histogram of $^{207}Pb/^{206}Pb$ dates (scale on left), neglecting associated error, and are included as a visual aid to the data patterns. On both graphs, replicate spot analyses and data with more than 5.5% discordance were not plotted.

Sample 05RAYAH194A2, sillimanite-biotite psammitic schist (Northern Chantrey group, lower marker unit)

In plane light microscopy, the zircon population is dominantly light to dark brown, with many grains appearing slightly turbid (Fig. 11a). The population is dominated by equant, anhedral, light to medium brown grains (*see* grain 85 in Fig. 11). Backscattered-electron imaging reveals oscillatory zoning in most grains, although some appear homogeneous or contain sector zoning (Fig. 11b). There is also a subpopulation that is elongate, subhedral, light to medium brown, clear to turbid, and occasionally displays one fractured end. This subpopulation of grains dominantly displays broad concentric zoning in BSE images (grain 15, Fig. 11b).

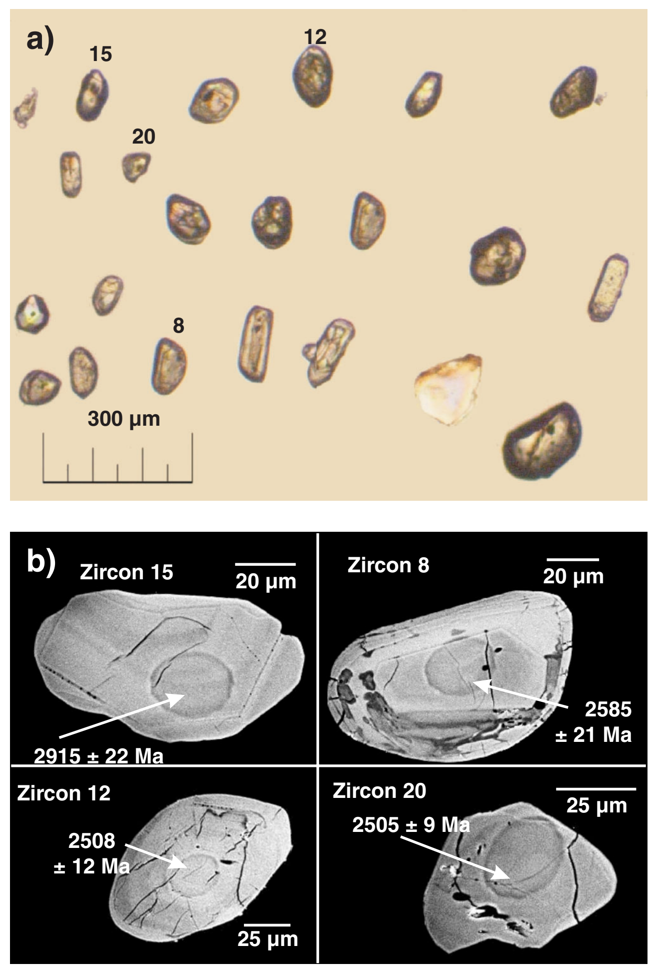

Figure 9. a) Transmitted-light image of detrital zircon grains picked from sample 05RAYAH192A2, a sillimanite-biotite psammitic schist from the Northern Chantrey group. Numbers in figure refer to the grain-identification numbers used during SHRIMP analysis and referred to in the text. **b)** Backscattered-electron images of a representative selection of zircon grains. The internal zoning of the zircon grains and the pit left by the ion beam appear in the images. The $^{207}Pb/^{206}Pb$ dates are reported by the analytical site (*see* Appendix A for details). Zircon numbers correspond to spot numbers listed in Appendix A.

Ninety-six analyses were conducted on 92 different zircon grains. The results are plotted on a concordia diagram (Fig. 12a) and a cumulative probability curve (Fig. 12b). Ages range from 3422 Ma to 2456 Ma. The majority of data are less than 5% discordant. Prominent age modes are evident at 2600 Ma (n ≅ 14), 2700 Ma (n ≅ 6), 2755 Ma (n ≅ 7), 2810 Ma (n ≅ 5), 2900 Ma (n ≅ 3), and 3130 Ma (n ≅ 3). Multiple analysis of the youngest grain yielded a weighted mean $^{207}Pb/^{206}Pb$ age of 2456 ± 13 Ma (2σ error, n = 5; grain 15; Fig. 12a; MSWD = 0.60; probability of fit = 66%), interpreted as a maximum depositional age of the unit.

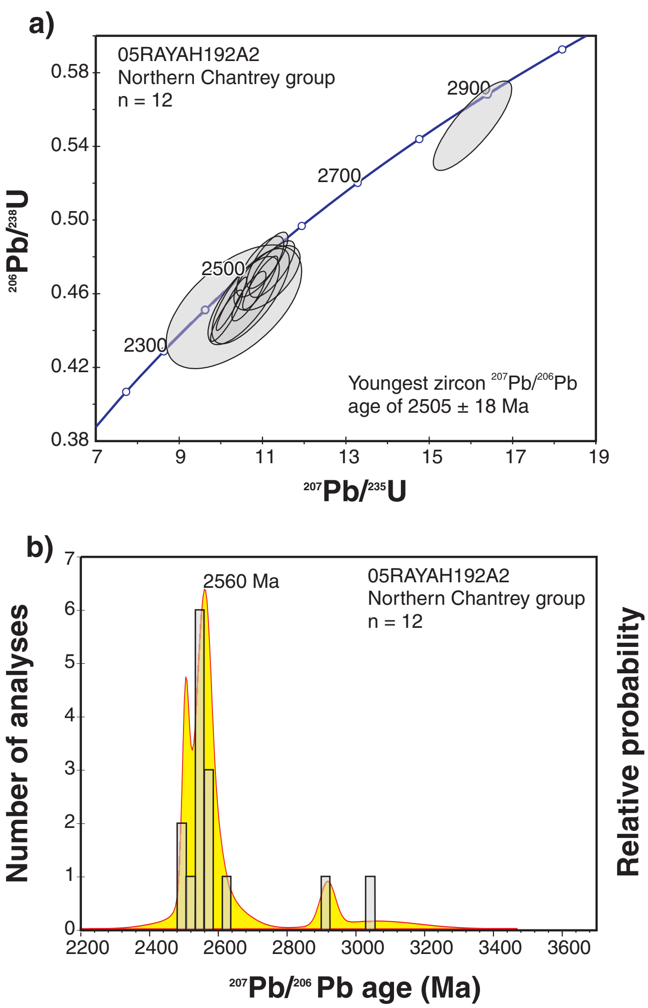

Figure 10. a) Concordia diagram of U-Pb results from sample 05RAYAH192A2, a sillimanite-biotite psammitic schist from the Northern Chantrey group. Error ellipses are at 2σ Level. **b)** Cumulative probability curve where the curve represents a weighted cell-less summed probability histogram, into which errors of individual analysis have been incorporated. Grey columns represent a frequency histogram of $^{207}Pb/^{206}Pb$ dates (scale on left), neglecting associated error, and are included as a visual aid to the data patterns. On both graphs, data with more than 5% discordance were not plotted.

DISCUSSION

Detrital zircon analyses from the muscovite-biotite schist of the Barclay belt constrain the maximum age of deposition to 2764 Ma or later. There are no robust geochronological constraints on the minimum age of deposition. At the map scale, the supracrustal rocks of the Barclay belt were likely intruded by monzogranite that is interpreted as being part of the regionally widespread, ca. 2.6 Ga plutonic suite. In the sequence where the sample was collected, the intrusive contact with the surrounding granite is not exposed. There are no dykes of the granite in the metasedimentary rocks, there are no rafts of the metasedimentary rocks in the granite, and there are no granite fragments in the metasedimentary rocks, leaving the relationship unconstrained. The detrital grain

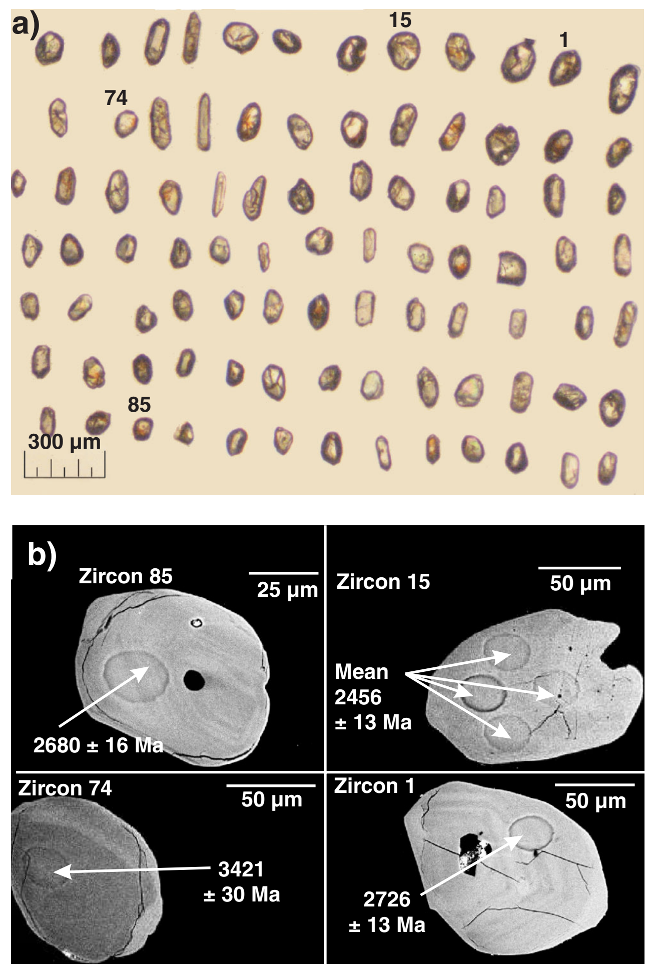

Figure 11. a) Transmitted-light image of detrital zircon grains picked from sample 05RAYAH194A2, a sillimanite-biotite psammitic schist from the Northern Chantrey group. Numbers in figure refer to the grain-identification numbers used during SHRIMP analysis and referred to in the text. **b)** Backscattered-electron images of a representative selection of zircon grains. The internal zoning of the zircon grains and the pit left by the ion beam appear in the images. The $^{207}Pb/^{206}Pb$ dates are reported by the analytical site (*see* Appendix A for details). Zircon numbers correspond to spot numbers listed in Appendix A.

signature is similar to that of other Archean supracrustal belts elsewhere in the Rae Domain, specifically the Prince Albert Group of the Committee Bay belt (Skulski et al., 2003; T. Skulski, talk presented at Western Churchill Metallogeny Project Spring 2004 Meeting, Ottawa, Ontario, April 29–30, 2004; (http://ess.nrcan.gc.ca/2002_2006/nrd/wchurchill/project_8_2_pres_6_e.php [accessed February 15, 2006]). The Barclay belt sample differs in that zircon with ca. 2730–2710 Ma ages typical of magmatic rocks of the Prince Albert Group and Woodburn Lake group are not documented in this sample (Skulski et al., 2003; T. Skulski, talk presented at Western Churchill Metallogeny Project Spring 2004 Meeting, Ottawa, Ontario, April 29–30, 2004; (http://ess.nrcan.gc.ca/2002_2006/nrd/wchurchill/project_8_2_pres_6_e.php [accessed February 15, 2006])). Based on the present data set, the Barclay belt may be a distinct sequence that is older than the Prince Albert Group; however, the absence of ca. 2.73–2.71 Ma zircon ages can also be interpreted to indicate that the sample is from the lowest, and hence oldest part of the supracrustal belt, and predates most of the 2.73–2.71 Ma magmatic rocks.

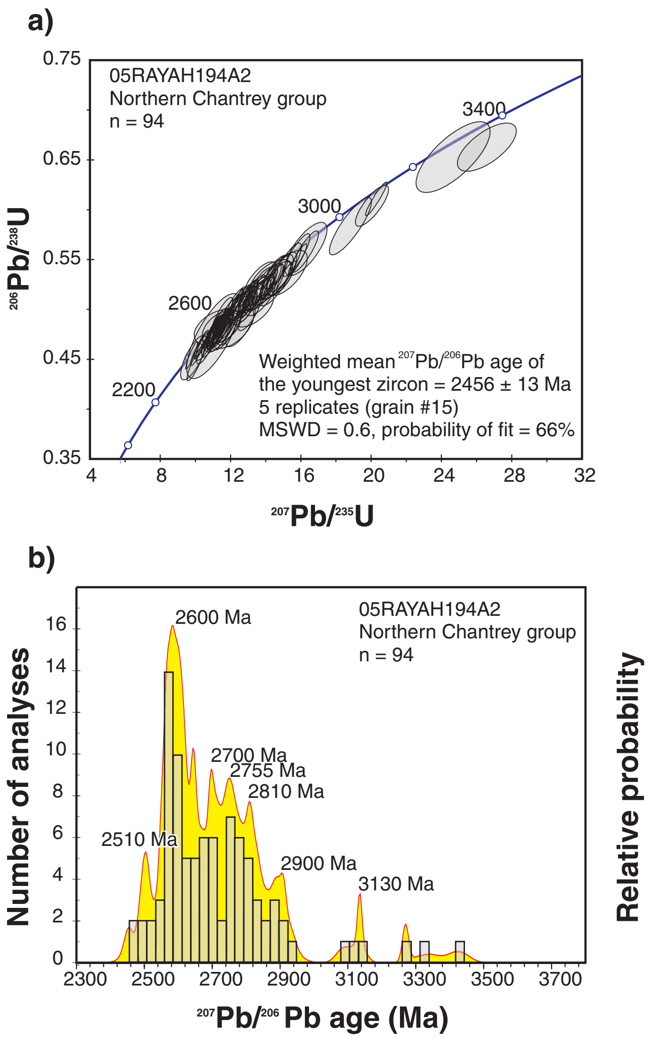

Figure 12. a) Concordia diagram of U-Pb results from sample 05RAYAH194A2, a sillimanite-biotite psammitic schist from the Northern Chantrey group. Error ellipses are at 2σ level. **b)** Cumulative probability curve where the curve represents a weighted cell-less summed probability histogram, into which errors of individual analysis have been incorporated. Grey columns represent a frequency histogram of $^{207}Pb/^{206}Pb$ dates (scale on left), neglecting associated error, and are included as a visual aid to the data patterns. On both graphs, replicate spot analyses and data with more than 5.5% discordance were not plotted.

Archean Mary River Group is preserved dominantly on Baffin Island, is interpreted as being correlative with the Prince Albert Group (Jackson, 2000; Young et al., 2004), and may also be correlative with the Barclay belt. The Mary River Group is similar to the Barclay belt schist in that it preserves felsic volcanic rocks with a comparable age range of inherited zircon (Bethune and Scammell, 2003), and a metasandstone with a detrital grain signature dominated by ca. 2860 Ma zircon grains (N. Wodicka, unpub. data, 2005). The zircon ages are similar to those preserved in the Barclay belt schist. The Barclay belt likely reflects an Archean volcano-sedimentary sequence dominated by metabasalt and psammitic schist. There are minor komatiite flows (preserving very rare spinifex texture) occurring in similar supracrustal rocks in the very northwest corner of the Darby Lake map area (NTS 56 N; Sandeman et al. (2005)), immediately along strike to the southwest of the present geochronology sampling site. These supracrustal rocks represent the southernmost extension of the rocks Frisch (2000) referred to as Barclay belt. On the basis of correlations with rocks in the Committee Bay belt to the southeast, Sandeman et al. (2005) suggested that these supracrustal rocks were contemporaneous with the Prince Albert Group.

The maximum depositional ages determined for the psammitic layers in the Northern Chantrey group indicate that the sequence is Paleoproterozoic, and thus potentially correlative with other Rae Domain cover sequences, such as the Amer, Ketyet River, and Piling groups. Detrital zircon studies of the Amer, Ketyet River, and Piling groups demonstrate that the stratigraphically lowest parts of these sequences contain dominantly Archean zircon older than 2.6 Ga of probable local derivation (R.H. Rainbird, W.J. Davis, and S.J. Pehrsson, talk presented at Western Churchill Metallogeny Project Spring 2004 Meeting, Ottawa, Ontario, April 29–30, 2004; Geological Survey of Canada; (http://ess.nrcan.gc.ca/2002_2006/nrd/wchurchill/project_8_2_pres_21_e.php [accessed February 15, 2006); Rainbird et al. 2005; St-Onge et al., 2005a, b; W.J. Davis and R. Rainbird unpub. data, 2006). A broader and more diverse age population is characteristic of the higher stratigraphic parts of the sequences. In particular, they contain significant 2.4–1.9 Ga zircon populations interpreted to be derived from sources in the western Rae Domain and Taltson-Thelon zone (R.H. Rainbird, W.J. Davis, and S.J. Pehrsson, talk presented at Western Churchill Metallogeny Project Spring 2004 Meeting, Ottawa, Ontario, April 29–30, 2004; Geological Survey of Canada; (http://ess.nrcan.gc.ca/2002_2006/nrd/wchurchill/project_8_2_pres_21_e.php [accessed February 15, 2006]); Rainbird et al., 2005; St-Onge et al., 2005a, b; W.J. Davis and R. Rainbird unpub. data, 2006). Detrital zircon of this age is not documented in the samples from the Boothia mainland area, suggesting that the sequence would be correlative with the lower parts of the Amer, Ketyet River, and Piling groups. This is consistent with the proximity of the samples to the basement-cover contact. The two Proterozoic samples presented here represent the only detrital zircon analysis yet performed on the Chantrey Group.

ACKNOWLEDGMENTS

The Boothia Peninsula Integrated Geoscience Project was funded by the Geological Survey of Canada's Northern Resources Development Program, the Canada-Nunavut Geoscience Office, and the Polar Continental Shelf Project. Thank you to Mike Young for volunteering to draft Figure 2. Special thanks to the whole field crew and for field visits by Rob Berman, Bill Davis, Ernst Schetselaar, and Dave Scott. Thanks to the field cook, Dorothy Edwards. Thank you to helicopter pilots Terry Halton and Colin Lavalle with Universal Helicopters for a safe and productive summer of flying. Excellent Twin Otter service was supplied through Borek Air under a Polar Continental Shelf Project contract. Charlie Cahill at Cap Enterprises provided expediting services out of Gjoa Haven. This manuscript benefited from thoughtful reviews by N. Wodicka.

REFERENCES

Berman, R.G., Sanborn-Barrie, M., Stern, R.A., and Carson, C.J.
2005: Tectonometamorphism at ca. 2.35 and 1.85 Ga in the Rae Domain, western Churchill Province, Nunavut, Canada; insights from structural, metamorphic and in situ geochronological analysis of the southwestern Committee Bay Belt; The Canadian Mineralogist, v. 43, p. 409–442.

Bethune, K. and Scammell, R.J.
2003: Geology, geochronology, and geochemistry of Archean rocks in the Eqe Bay area, north-central Baffin Island, Canada: constraints on the depositional and tectonic history of the Mary River Group of northeastern Rae Province; Canadian Journal of Earth Sciences, v. 40, p. 1137–1167.

Bostock, H.H. and van Breemen, O.
1994: Ages of detrital and metamorphic zircons and monazites from a pre-Taltson magmatic zone basin at the western margin of Rae Province; Canadian Journal of Earth Sciences, v. 31, p. 1353–1364.

Coyle, M., Dumont, R., Kiss, F., and Potvin, J.
2005a: First vertical derivative of the magnetic field, 57 A/NW, Nunavut / Dérivée premiPre verticale du champ magnétique, 57 A/NW, Nunavut; Geological Survey of Canada, Open File 4904, 1 sheet.

Coyle, M., Dumont, R., Kiss, F., and Potvin, J. (continued)
2005b: First vertical derivative of the magnetic field, 57 A/SW, Nunavut / Dérivée premiPre verticale du champ magnétique, 57 A/SW, Nunavut; Geological Survey of Canada, Open File 4907, 1 sheet.
2005c: First vertical derivative of the magnetic field, 57 B/NE, Nunavut / Dérivée premiPre verticale du champ magnétique, 57 B/NE, Nunavut; Geological Survey of Canada, Open File 4903, 1 sheet.
2005d: First vertical derivative of the magnetic field, 57 B/NW, Nunavut / Dérivée premiPre verticale du champ magnétique, 57 B/NW, Nunavut; Geological Survey of Canada, Open File 4902, 1 sheet.
2005e: First vertical derivative of the magnetic field, 57 B/SE, Nunavut / Dérivée premiPre verticale du champ magnétique, 57 B/SE, Nunavut; Geological Survey of Canada, Open File 4906, 1 sheet.
2005f: First vertical derivative of the magnetic field, 57 B/SW, Nunavut / Dérivée premiPre verticale du champ magnétique, 57 B/SW, Nunavut; Geological Survey of Canada, Open File 4905, 1 sheet.
2005g: First vertical derivative of the magnetic field, 57 C/NE, Nunavut / Dérivée premiPre verticale du champ magnétique, 57 C/NE, Nunavut; Geological Survey of Canada, Open File 4897, 1 sheet.
2005h: First vertical derivative of the magnetic field, 57 C/SE, Nunavut / Dérivée premiPre verticale du champ magnétique, 57 C/SE, Nunavut; Geological Survey of Canada, Open File 4900, 1 sheet.
2005i: First vertical derivative of the magnetic field, 57 C/SW, Nunavut / Dérivée premiPre verticale du champ magnétique, 57 C/SW, Nunavut; Geological Survey of Canada, Open File 4899, 1 sheet.
2005j: First vertical derivative of the magnetic field, 57 D/NW, Nunavut / Dérivée premiPre verticale du champ magnétique, 57 D/NW, Nunavut; Geological Survey of Canada, Open File 4898, 1 sheet.
2005k: First vertical derivative of the magnetic field, 57 D/SW, Nunavut / Dérivée premiPre verticale du champ magnétique, 57 D/SW, Nunavut; Geological Survey of Canada, Open File 4901, 1 sheet.
2005l: Residual total magnetic field, 57 A/NW, Nunavut / Composante résiduelle du champ magnétique total, 57 A/NW, Nunavut; Geological Survey of Canada, Open File 4915, 1 sheet.
2005m: Residual total magnetic field, 57 A/SW, Nunavut / Composante résiduelle du champ magnétique total, 57 A/SW, Nunavut; Geological Survey of Canada, Open File 4918, 1 sheet.
2005n: Residual total magnetic field, 57 B/NE, Nunavut / Composante résiduelle du champ magnétique total, 57 B/NE, Nunavut; Geological Survey of Canada, Open File 4914, 1 sheet.
2005o: Residual total magnetic field, 57 B/NW, Nunavut / Composante résiduelle du champ magnétique total, 57 B/NW, Nunavut; Geological Survey of Canada, Open File 4913, 1 sheet.
2005p: Residual total magnetic field, 57 B/SE, Nunavut / Composante résiduelle du champ magnétique total, 57 B/SE, Nunavut; Geological Survey of Canada, Open File 4917, 1 sheet.
2005q: Residual total magnetic field, 57 B/SW, Nunavut / Composante résiduelle du champ magnétique total, 57 B/SW, Nunavut; Geological Survey of Canada, Open File 4916, 1 sheet.

Coyle, M., Dumont, R., Kiss, F., and Potvin, J. (continued)
2005r: Residual total magnetic field, 57 C/NE, Nunavut / Composante résiduelle du champ magnétique total, 57 C/NE, Nunavut; Geological Survey of Canada, Open File 4908, 1 sheet.
2005s: Residual total magnetic field, 57 C/SE, Nunavut / Composante résiduelle du champ magnétique total, 57 C/SE, Nunavut; Geological Survey of Canada, Open File 4911, 1 sheet.
2005t: Residual total magnetic field, 57 C/SW, Nunavut / Composante résiduelle du champ magnétique total, 57 C/SW, Nunavut; Geological Survey of Canada, Open File 4910, 1 sheet.
2005u: Residual total magnetic field, 57 D/NW, Nunavut / Composante résiduelle du champ magnétique total, 57 D/NW, Nunavut; Geological Survey of Canada, Open File 4909, 1 sheet.
2005v: Residual total magnetic field, 57 D/SW, Nunavut / Composante résiduelle du champ magnétique total, 57 D/SW, Nunavut; Geological Survey of Canada, Open File 4912, 1 sheet.

Cumming, G.L. and Richards, J.R.
1975: Ore lead in a continuously changing Earth; Earth and Planetary Science Letters, v. 28, p. 155–171.

Frisch, T.
1982: Precambrian geology of the Prince Albert Hills, western Melville Peninsula, Northwest Territories; Geological Survey of Canada, Bulletin 346, 70 p.
2000: Precambrian geology of Ian Calder Lake, Cape Barclay, and part of Darby Lake map areas, south-central Nunavut; Geological Survey of Canada, Bulletin 542, 51 p.

Gibb, R.A. and Walcott, R.I.
1971: A Precambrian suture in the Canadian Shield; Earth and Planetary Science Letters, v. 10, p. 417–422.

Henderson, J.R.
1983: Structure and metamorphism of the Aphebian Penrhyn Group and its Archean basement complex in the Lyon Inlet area, Melville Peninsula, District of Franklin; Geological Survey of Canada, Bulletin 324, 50 p.

Heywood, W.W.
1961: Geological notes, northern District of Keewatin; Geological Survey of Canada, Paper 61-18, 9 p.

Hoffman, P.F.
1988: United plates of America, the birth of a craton; early Proterozoic assembly and growth of Laurentia; Annual Review of Earth and Planetary Sciences, v. 16, p. 543–603.
1990: Subdivision of the Churchill Province and extent of the Trans-Hudson Orogen; *in* The early Proterozoic Trans-Hudson Orogen of North America, (ed.) J.F. Lewry and M.R. Stauffer; Geological Association of Canada, Special Paper 37, p. 5–39.

Jackson, G.D.
2000: Geology of the Clyde-Cockburn Land Map area, north-central Baffin Island, Nunavut; Geological Survey of Canada, Memoir 440, 303 p.

Kraft, J.
2006: Petrology, geochronology and tectonometamorphism of the Paleoproterozoic Northern Chantrey Group, northern Rae Domain, Churchill Province, Nunavut; B.Sc. thesis, University of Alberta, Edmonton, Alberta, 66 p.

LeCheminant, A.N. and Heaman, L.M.
1989: Mackenzie igneous events, Canada; middle Proterozoic hotspot magmatism associated with ocean opening; Earth and Planetary Science Letters, v. 96, p. 38–48.

LeCheminant, A.N. and Roddick, J.C.
1991: U-Pb zircon evidence for widespread 2.6 Ga felsic magmatism in the central District of Keewatin, N.W.T.; *in* Radiogenic Age and Isotopic Studies, Report 4: Geological Survey of Canada, Paper 90-2, p. 91–99.

Ludwig, K.R.
2003: Isoplot 3.0, a geochronological toolkit for Microsoft Excel; Berkeley Geochronology Center, Special Publication No. 4, p. 70.

McDonough, M.R., McNicoll, V.J., Schetselaar, E.M., and Grover, T.W.
2000: Geochronological and kinematic constraints on crustal shortening and escape in a two-sided oblique-slip collisional and magmatic orogen, Paleoproterozoic Taltson magmatic zone, northeastern Alberta; Canadian Journal of Earth Sciences, v. 37, p. 1549–1573.

McNicoll, V.J., Theriault, R.J., and McDonough, M.R.
2000: Taltson basement gneissic rocks: U-Pb and Nd isotopic constraints on the basement to the Paleoproterozoic Taltson magmatic zone, northeastern Alberta; Canadian Journal of Earth Sciences, v. 37, p. 1575–1596.

Patterson, J.G.
1986: The Amer Belt; remnant of an Aphebian foreland fold and thrust belt; Canadian Journal of Earth Sciences, v. 23, p. 2012–2023.

Peterson, T.D., Van Breemen, O., Sandeman, H., and Cousens, B.
2002: Proterozoic (1.85-1.75 Ga) igneous suites of the Western Churchill Province: granitoid and ultrapotassic magmatism in a reworked Archean hinterland; Precambrian Research, v. 119, p. 73–100.

Rainbird, R.H., Davis, W.J., Pehrsson, S.J., and Wodicka, N.
2005: The Paleoproterozoic cover sequences of the Western Churchill Province: from the break-up of Kenorland to the assembly of Nuna; *in* Abstracts Volume, Geological Association of Canada-Mineralogical Association of Canada-Canadian Society of Petroleum Geologists-Canadian Society of Soil Science Joint Meeting, May 15–18, 2005, Halifax, Nova Scotia, v. 30, p. 162.

Sandeman, H.A., Schultz, M., and Rubingh, K.
2005: Results of bedrock mapping of the Darby Lake–Arrowsmith River north map areas, central Rae Domain, Nunavut; Geological Survey of Canada, Current Research 2005-C2, 11 p.

Scott, D.J., St-Onge, M.R., and Corrigan, D.
2002: Geology of the Paleoproterozoic Piling Group and underlying Archean gneiss, central Baffin Island, Nunavut; Geological Survey of Canada, Current Research 2002-C17, 10 p.

Skulski, T., Sandeman, H., Sanborn-Barrie, M., MacHattie, T., Young, M., Carson, C., Berman, R., Brown, J., Rayner, N., Panagapko, D., Byrne, D., and Deyell, C.
2003: Bedrock geology of the Ellice Hills map area and new constraints on the regional geology of the Committee Bay area, Nunavut; Geological Survey of Canada, Current Research 2003-C22, 11 p.

St-Onge, M.R., Scott, D.J., Corrigan, D., and Wodicka, N.
2005a: Geology, Ikpik Bay, Baffin Island, Nunavut; Geological Survey of Canada, Map 2077A, scale 1:100 000.
2005b: Geology, Dewar Lakes, Baffin Island, Nunavut; Geological Survey of Canada, Map 2082A, scale 1:100 000.

Stern, R.A.
1997: The GSC Sensitive High Resolution Ion Microprobe (SHRIMP): analytical techniques of zircon U-Th-Pb age determinations and performance evaluation; Geological Survey of Canada, Current Research 1997-F, p. 1–31.

Stern, R.A. and Amelin, Y.
2003: Assessment of errors in SIMS zircon U-Pb geochronology using a natural zircon standard and NIST SRM 610 glass; Chemical Geology, v. 197, p. 111–146.

Tella, S.
1994: Geology, Amer Lake (66 H), Deep Rose Lake (66 G) and parts of Pelly Lake (66 F); Geological Survey of Canada, Open File 2969, scale 1:250 000.

Tremblay, T.
2005: Ice movement and glacial transport studies, southern Boothia Peninsula (NTS map areas 57A and 57B), Nunavut; *in* Proceedings with Abstract; 33rd Annual Yellowknife Geoscience Forum, November 16–18, 2005; Northwest Territories Geoscience Office, Yellowknife, Northwest Territories, p. 76.

Young, M.D., Sandeman, H.A., Berniolles, F., and Gertzbein, P.M.
2004: A preliminary stratigraphic and structural geology framework for the Archean Mary River Group, northern Baffin Island, Nunavut; Geological Survey of Canada, Current Research 2004-C1, 14 p.

Zaleski, E., Davis, W.J., and Sandeman, H.A.
2001: Continental extension, mantle magmas & basement/cover relationships; *in* Extended Abstracts, 4th International Archean Symposium 2001; (ed.) K.F. Cassidy, J.M. Dunphy, and M.J. van Kranendonk; Australian Geological Survey Organisation, Report 2001/37, p. 374–376.

Geological Survey of Canada Project Y16

APPENDIX A

Uranium-lead SHRIMP zircon data for **a)** muscovite-biotite psammitic schist (05RAYAH184A3) from the Barclay belt, **b)** sillimanite-biotite psammitic schist (05RAYAH192A2) from the Northern Chantrey group, and **c)** sillimanite-biotite psammitic schist (05RAYAH194A2) from the Northern Chantrey group.

Spot[a]	U (ppm)	Th (ppm)	Th/U	Pb* (ppm)	^{204}Pb (ppb)	^{204}Pb/^{206}Pb	f(206)^{204} [c]	^{208*}Pb/^{206*}Pb	^{207*}Pb/^{235}U	^{206*}Pb/^{238}U	Corr Coeff[d]	^{207*}Pb/^{206*}Pb	Apparent ages (Ma)[b] ^{206}Pb/^{238}U	Apparent ages (Ma)[b] ^{207}Pb/^{235}U	Apparent ages (Ma)[b] ^{207}Pb/^{206}Pb	Disc. (%)[e]
a) Sample 05RAYAH184A3 - muscovite-biotite psammitic schist from the Barclay belt UTM: 489037E, 7545066N																
8799-31.1	60	49	0.851	39	12	0.000426 ± 0.000117	0.007380	0.2297 ± 0.0066	14.135 ± 0.306	0.5311 ± 0.0075	0.737	0.1930 ± 0.0029	2746 ± 32	2759 ± 21	2768 ± 24	0.8
8799-31.2.2	122	80	0.682	77	37	0.000663 ± 0.000098	0.011490	0.1887 ± 0.0062	14.273 ± 0.318	0.5292 ± 0.0096	0.878	0.1956 ± 0.0021	2738 ± 41	2768 ± 21	2790 ± 18	1.9
8799-31.2.3	112	73	0.679	68	36	0.000728 ± 0.000081	0.012620	0.1854 ± 0.0056	13.678 ± 0.361	0.5125 ± 0.0117	0.914	0.1936 ± 0.0021	2667 ± 50	2728 ± 25	2773 ± 18	3.8
8799-31.2.4	102	64	0.652	62	33	0.000727 ± 0.000087	0.012600	0.1907 ± 0.0041	13.406 ± 0.384	0.5086 ± 0.0130	0.935	0.1912 ± 0.0020	2651 ± 56	2709 ± 27	2752 ± 17	3.7
8799-31.4.2	70	55	0.816	40	39	0.001359 ± 0.000255	0.023550	0.2283 ± 0.0103	12.722 ± 0.395	0.4627 ± 0.0089	0.710	0.1994 ± 0.0044	2451 ± 39	2659 ± 30	2821 ± 36	13.1
8799-31.4.3	62	50	0.823	35	27	0.001078 ± 0.000153	0.018680	0.2372 ± 0.0069	12.365 ± 0.382	0.4545 ± 0.0116	0.882	0.1973 ± 0.0029	2415 ± 51	2632 ± 29	2804 ± 24	13.9
8799-31.4.4	56	44	0.805	31	31	0.001402 ± 0.000223	0.024300	0.2229 ± 0.0112	11.821 ± 0.432	0.4457 ± 0.0124	0.833	0.1924 ± 0.0039	2376 ± 56	2590 ± 35	2763 ± 34	14.0
8799-44.1	105	116	1.141	70	66	0.001412 ± 0.000275	0.024470	0.3246 ± 0.0114	13.627 ± 0.443	0.5099 ± 0.0098	0.680	0.1938 ± 0.0047	2656 ± 42	2724 ± 31	2775 ± 40	4.3
8799-44.1.2	110	123	1.149	63	48	0.001126 ± 0.000110	0.019520	0.3183 ± 0.0072	11.621 ± 0.265	0.4384 ± 0.0080	0.864	0.1923 ± 0.0022	2343 ± 36	2574 ± 22	2762 ± 19	15.1
8799-44.1.3	113	124	1.135	63	43	0.001012 ± 0.000138	0.017540	0.3165 ± 0.0073	11.441 ± 0.346	0.4300 ± 0.0097	0.817	0.1930 ± 0.0034	2306 ± 44	2560 ± 29	2768 ± 29	16.7
8799-44.5.2	104	86	0.859	59	54	0.001313 ± 0.000177	0.022750	0.2642 ± 0.0092	12.049 ± 0.367	0.4491 ± 0.0102	0.816	0.1946 ± 0.0035	2391 ± 45	2608 ± 29	2781 ± 29	14.0
8799-44.5.3	101	84	0.861	56	49	0.001246 ± 0.000159	0.021590	0.2586 ± 0.0081	11.690 ± 0.349	0.4443 ± 0.0107	0.868	0.1908 ± 0.0029	2370 ± 48	2580 ± 28	2749 ± 25	13.8
8799-62.1	57	37	0.668	35	64	0.002440 ± 0.000265	0.042290	0.1794 ± 0.0122	13.650 ± 0.428	0.5090 ± 0.0086	0.637	0.1945 ± 0.0047	2652 ± 37	2726 ± 30	2781 ± 41	4.6
8799-65.1	72	78	1.122	48	66	0.002017 ± 0.000188	0.034960	0.3167 ± 0.0127	13.946 ± 0.355	0.5113 ± 0.0079	0.698	0.1978 ± 0.0036	2662 ± 34	2746 ± 24	2808 ± 30	5.2
8799-19.1	85	40	0.481	53	7	0.000175 ± 0.000088	0.003030	0.1355 ± 0.0038	14.813 ± 0.280	0.5373 ± 0.0074	0.808	0.2000 ± 0.0023	2772 ± 31	2803 ± 18	2826 ± 18	1.9
8799-26.1	39	17	0.443	24	11	0.000630 ± 0.000176	0.010910	0.1159 ± 0.0074	14.745 ± 0.410	0.5344 ± 0.0082	0.649	0.2001 ± 0.0043	2760 ± 35	2799 ± 27	2827 ± 35	2.4
8799-16.1	83	27	0.329	50	8	0.000211 ± 0.000067	0.003650	0.0874 ± 0.0033	15.131 ± 0.294	0.5453 ± 0.0089	0.894	0.2012 ± 0.0018	2806 ± 37	2824 ± 19	2836 ± 14	1.1
8799-41.1	63	29	0.480	39	12	0.000412 ± 0.000095	0.007130	0.1333 ± 0.0050	15.047 ± 0.276	0.5394 ± 0.0069	0.778	0.2023 ± 0.0024	2781 ± 29	2818 ± 18	2845 ± 19	2.3
8799-48.1	74	40	0.554	47	87	0.002424 ± 0.000236	0.042010	0.1535 ± 0.0099	15.080 ± 0.416	0.5395 ± 0.0079	0.629	0.2027 ± 0.0044	2781 ± 33	2820 ± 27	2848 ± 36	2.3
8799-40.1	99	46	0.481	61	12	0.000251 ± 0.000049	0.004360	0.1343 ± 0.0027	15.117 ± 0.226	0.5402 ± 0.0066	0.882	0.2030 ± 0.0014	2784 ± 28	2823 ± 14	2850 ± 12	2.3
8799-50.1	113	86	0.783	76	67	0.001227 ± 0.000137	0.021270	0.2106 ± 0.0075	15.481 ± 0.373	0.5517 ± 0.0096	0.800	0.2035 ± 0.0030	2832 ± 40	2845 ± 23	2855 ± 24	0.8
8799-72.1	146	70	0.494	92	40	0.000583 ± 0.000127	0.010100	0.1292 ± 0.0053	15.431 ± 0.297	0.5496 ± 0.0070	0.746	0.2036 ± 0.0026	2824 ± 29	2842 ± 19	2855 ± 21	1.1
8799-52.1	235	112	0.494	125	71	0.000761 ± 0.000173	0.013190	0.1555 ± 0.0067	12.735 ± 0.289	0.4535 ± 0.0070	0.765	0.2037 ± 0.0030	2411 ± 31	2660 ± 22	2856 ± 24	15.6
8799-63.1	63	31	0.505	40	57	0.001868 ± 0.000185	0.032380	0.1408 ± 0.0080	15.390 ± 0.371	0.5459 ± 0.0084	0.724	0.2045 ± 0.0034	2808 ± 35	2840 ± 23	2862 ± 28	1.9
8799-53.1	55	26	0.481	34	64	0.002452 ± 0.000489	0.042490	0.1380 ± 0.0193	15.043 ± 0.799	0.5332 ± 0.0126	0.549	0.2046 ± 0.0092	2755 ± 53	2818 ± 52	2863 ± 75	3.8
8799-10.1	51	18	0.358	31	9	0.000382 ± 0.000129	0.006620	0.0960 ± 0.0053	15.534 ± 0.324	0.5488 ± 0.0078	0.763	0.2053 ± 0.0028	2820 ± 33	2849 ± 20	2869 ± 22	1.7
8799-37.1	151	88	0.602	95	14	0.000210 ± 0.000038	0.003640	0.1713 ± 0.0027	15.199 ± 0.293	0.5292 ± 0.0076	0.814	0.2083 ± 0.0024	2738 ± 32	2828 ± 19	2892 ± 18	5.3
8799-2.1	23	10	0.448	15	3	0.000291 ± 0.000165	0.005040	0.1295 ± 0.0092	16.039 ± 0.407	0.5579 ± 0.0097	0.766	0.2085 ± 0.0034	2858 ± 40	2879 ± 25	2894 ± 27	1.3
8799-11.1	76	28	0.384	48	6	0.000159 ± 0.000065	0.002750	0.1060 ± 0.0031	16.175 ± 0.292	0.5621 ± 0.0078	0.841	0.2087 ± 0.0021	2875 ± 32	2887 ± 17	2895 ± 16	0.7
8799-79.1	55	12	0.229	34	54	0.002002 ± 0.000205	0.034700	0.0666 ± 0.0105	15.941 ± 0.453	0.5521 ± 0.0094	0.689	0.2094 ± 0.0044	2834 ± 39	2873 ± 28	2901 ± 34	2.3
8799-43.1	65	23	0.369	42	36	0.001123 ± 0.000194	0.019460	0.1166 ± 0.0086	16.151 ± 0.573	0.5583 ± 0.0103	0.618	0.2098 ± 0.0059	2859 ± 43	2886 ± 34	2904 ± 46	1.5
8799-25.1	82	27	0.337	51	8	0.000199 ± 0.000054	0.003440	0.0906 ± 0.0026	16.029 ± 0.264	0.5537 ± 0.0075	0.877	0.2100 ± 0.0017	2841 ± 31	2879 ± 16	2905 ± 13	2.2
8799-47.1	129	43	0.344	81	10	0.000164 ± 0.000059	0.002840	0.0947 ± 0.0028	16.353 ± 0.235	0.5585 ± 0.0063	0.852	0.2124 ± 0.0016	2861 ± 26	2898 ± 14	2924 ± 12	2.2
8799-3.1	101	132	1.347	78	7	0.000150 ± 0.000055	0.002590	0.3692 ± 0.0037	16.631 ± 0.260	0.5665 ± 0.0069	0.845	0.2129 ± 0.0018	2893 ± 28	2914 ± 15	2928 ± 14	1.2
8799-18.1	58	19	0.338	38	10	0.000353 ± 0.000111	0.006120	0.0869 ± 0.0046	17.010 ± 0.362	0.5783 ± 0.0076	0.708	0.2133 ± 0.0032	2942 ± 31	2935 ± 21	2931 ± 25	0.4
8799-4.1	70	36	0.534	46	3	0.000097 ± 0.000073	0.001670	0.1475 ± 0.0036	16.472 ± 0.298	0.5595 ± 0.0077	0.827	0.2135 ± 0.0022	2865 ± 32	2905 ± 17	2932 ± 17	2.3
8799-29.1	80	36	0.466	51	10	0.000269 ± 0.000057	0.004670	0.1228 ± 0.0029	16.605 ± 0.293	0.5567 ± 0.0085	0.918	0.2163 ± 0.0015	2853 ± 35	2912 ± 17	2954 ± 11	3.4
8799-64.1	434	147	0.351	267	69	0.000339 ± 0.000030	0.005880	0.0947 ± 0.0016	16.339 ± 0.267	0.5450 ± 0.0076	0.907	0.2174 ± 0.0015	2804 ± 32	2897 ± 16	2962 ± 11	5.3
8799-54.1	82	52	0.650	56	67	0.001640 ± 0.000155	0.028430	0.1741 ± 0.0095	16.912 ± 0.496	0.5631 ± 0.0075	0.558	0.2178 ± 0.0053	2880 ± 31	2930 ± 29	2965 ± 40	2.9
8799-73.1	75	104	1.436	59	47	0.001274 ± 0.000154	0.022070	0.4013 ± 0.0075	17.047 ± 0.413	0.5676 ± 0.0099	0.793	0.2178 ± 0.0032	2898 ± 41	2938 ± 24	2965 ± 24	2.3
8799-59.1	51	38	0.775	36	71	0.002657 ± 0.000243	0.046050	0.2076 ± 0.0103	17.574 ± 0.555	0.5842 ± 0.0118	0.726	0.2182 ± 0.0048	2966 ± 48	2967 ± 31	2967 ± 36	0.1
8799-61.1	105	84	0.832	76	52	0.000974 ± 0.000144	0.016880	0.2265 ± 0.0081	17.938 ± 0.406	0.5865 ± 0.0091	0.765	0.2218 ± 0.0033	2975 ± 37	2986 ± 22	2994 ± 24	0.6
8799-1.1	126	44	0.360	83	5	0.000084 ± 0.000027	0.001460	0.0961 ± 0.0022	17.757 ± 0.272	0.5794 ± 0.0074	0.887	0.2223 ± 0.0016	2946 ± 30	2977 ± 15	2997 ± 12	1.7
8799-21.1	37	34	0.946	28	6	0.000326 ± 0.000121	0.005640	0.2572 ± 0.0071	17.947 ± 0.456	0.5855 ± 0.0112	0.825	0.2223 ± 0.0032	2971 ± 46	2987 ± 25	2997 ± 23	0.9
8799-6.1	91	43	0.487	61	5	0.000115 ± 0.000037	0.001990	0.1326 ± 0.0023	17.594 ± 0.259	0.5724 ± 0.0074	0.923	0.2230 ± 0.0013	2917 ± 30	2968 ± 14	3002 ± 9	2.8
8799-32.1	92	61	0.685	65	10	0.000226 ± 0.000048	0.003920	0.1888 ± 0.0029	17.769 ± 0.295	0.5780 ± 0.0076	0.855	0.2230 ± 0.0019	2941 ± 31	2977 ± 16	3002 ± 14	2.1
8799-23.1	43	27	0.657	30	7	0.000337 ± 0.000095	0.005840	0.1803 ± 0.0077	17.905 ± 0.407	0.5818 ± 0.0093	0.784	0.2232 ± 0.0032	2956 ± 38	2985 ± 22	3004 ± 23	1.6
8799-20.1	25	12	0.505	18	7	0.000513 ± 0.000156	0.008900	0.1348 ± 0.0069	18.393 ± 0.430	0.5937 ± 0.0096	0.773	0.2247 ± 0.0034	3004 ± 39	3011 ± 23	3015 ± 24	0.3

APPENDIX A (cont.)

Spot[a]	U (ppm)	Th (ppm)	Th/U	Pb* (ppm)	^{204}Pb (ppb)	^{204}Pb/^{206}Pb	f(206)^{204} [c]	^{208*}Pb/^{206*}Pb	^{207*}Pb/^{235}U	^{206*}Pb/^{238}U	Corr Coeff[d]	^{207*}Pb/^{206*}Pb	Apparent ages (Ma)[b] ^{206}Pb/^{238}U	^{207}Pb/^{235}U	^{207}Pb/^{206}Pb	Disc. (%)[e]
8799-60.1	86	34	0.407	58	62	0.001406 ± 0.000188	0.024370	0.1051 ± 0.0083	18.222 ± 0.405	0.5850 ± 0.0081	0.714	0.2259 ± 0.0035	2969 ± 33	3002 ± 22	3023 ± 25	1.8
8799-39.1	16	6	0.368	11	10	0.001158 ± 0.000393	0.020070	0.1061 ± 0.0154	18.218 ± 0.695	0.5803 ± 0.0113	0.610	0.2277 ± 0.0069	2950 ± 46	3001 ± 37	3036 ± 50	2.8
8799-51.1	53	24	0.469	36	57	0.002071 ± 0.000197	0.035890	0.1378 ± 0.0086	18.252 ± 0.484	0.5793 ± 0.0097	0.719	0.2285 ± 0.0043	2946 ± 40	3003 ± 26	3042 ± 30	3.1
8799-46.1	54	49	0.926	41	57	0.001996 ± 0.000213	0.034600	0.2603 ± 0.0126	18.965 ± 0.680	0.5928 ± 0.0141	0.749	0.2320 ± 0.0056	3001 ± 57	3040 ± 35	3066 ± 39	2.1
8799-80.1	45	38	0.886	35	65	0.002678 ± 0.000266	0.046420	0.2469 ± 0.0133	19.970 ± 0.574	0.6013 ± 0.0102	0.681	0.2409 ± 0.0051	3035 ± 41	3090 ± 28	3126 ± 34	2.9
8799-5.1	128	45	0.367	91	10	0.000153 ± 0.000069	0.002650	0.0974 ± 0.0029	20.852 ± 0.315	0.6171 ± 0.0075	0.870	0.2451 ± 0.0018	3098 ± 30	3132 ± 15	3153 ± 12	1.7
8799-58.1	97	69	0.740	74	77	0.001466 ± 0.000121	0.025410	0.1903 ± 0.0054	21.397 ± 0.360	0.6194 ± 0.0076	0.807	0.2505 ± 0.0025	3108 ± 30	3157 ± 16	3188 ± 16	2.5
8799-24.1	213	110	0.534	160	9	0.000075 ± 0.000018	0.001300	0.1462 ± 0.0016	21.899 ± 0.296	0.6249 ± 0.0073	0.915	0.2542 ± 0.0014	3129 ± 29	3179 ± 13	3211 ± 9	2.5
8799-8.1	26	14	0.564	20	10	0.000663 ± 0.000227	0.011490	0.1451 ± 0.0104	22.461 ± 0.686	0.6406 ± 0.0118	0.696	0.2543 ± 0.0056	3191 ± 47	3204 ± 30	3212 ± 35	0.6
8799-34.1	99	80	0.833	81	14	0.000259 ± 0.000073	0.004490	0.2225 ± 0.0035	22.560 ± 0.341	0.6427 ± 0.0079	0.875	0.2546 ± 0.0019	3200 ± 31	3208 ± 15	3213 ± 12	0.4
8799-78.1	95	73	0.790	78	67	0.001239 ± 0.000120	0.021470	0.2128 ± 0.0058	22.592 ± 0.506	0.6432 ± 0.0094	0.739	0.2548 ± 0.0039	3201 ± 37	3210 ± 22	3215 ± 24	0.4
8799-57.1	54	47	0.888	44	74	0.002402 ± 0.000220	0.041630	0.2297 ± 0.0097	22.552 ± 0.712	0.6366 ± 0.0150	0.819	0.2569 ± 0.0047	3176 ± 59	3208 ± 31	3228 ± 29	1.6
8799-17.1	55	44	0.836	45	7	0.000250 ± 0.000075	0.004330	0.2336 ± 0.0050	22.875 ± 0.434	0.6338 ± 0.0093	0.840	0.2618 ± 0.0027	3165 ± 37	3222 ± 19	3257 ± 16	2.8
8799-36.1	91	68	0.773	75	8	0.000152 ± 0.000052	0.002640	0.2099 ± 0.0031	23.897 ± 0.326	0.6450 ± 0.0075	0.909	0.2687 ± 0.0015	3209 ± 30	3264 ± 13	3298 ± 9	2.7
8799-74.1	31	20	0.676	25	58	0.003198 ± 0.000346	0.055420	0.1911 ± 0.0155	23.887 ± 0.728	0.6407 ± 0.0106	0.641	0.2704 ± 0.0064	3192 ± 42	3264 ± 30	3308 ± 37	3.5
8799-56.1	49	23	0.481	39	50	0.001760 ± 0.000301	0.030510	0.1385 ± 0.0120	24.567 ± 0.884	0.6552 ± 0.0153	0.733	0.2720 ± 0.0067	3248 ± 60	3291 ± 36	3317 ± 39	2.1
8799-7.1	204	92	0.466	183	8	0.000061 ± 0.000015	0.001060	0.1253 ± 0.0012	31.949 ± 0.414	0.7197 ± 0.0088	0.974	0.3220 ± 0.0010	3495 ± 33	3549 ± 13	3579 ± 5	2.4
8799-33.1	115	41	0.371	103	12	0.000164 ± 0.000034	0.002850	0.0967 ± 0.0019	32.868 ± 0.525	0.7315 ± 0.0106	0.945	0.3259 ± 0.0017	3539 ± 39	3577 ± 16	3598 ± 8	1.6
8799-12.1	37	29	0.805	40	8	0.000296 ± 0.000068	0.005130	0.2139 ± 0.0041	40.163 ± 0.665	0.7961 ± 0.0113	0.908	0.3659 ± 0.0026	3775 ± 41	3775 ± 17	3774 ± 11	0.0
b) Sample 05RAYAH192A2 - Sillimanite-biotite psammitic schist from the Northern Chantrey group. UTM: 555299E, 7643741N																
8801-20.1	860	390	0.468	440	77	0.000230 ± 0.000021	0.003980	0.1389 ± 0.0024	10.366 ± 0.148	0.4564 ± 0.0058	0.936	0.1647 ± 0.0008	2424 ± 26	2468 ± 13	2505 ± 9	3.2
8801-12.1	514	290	0.583	266	57	0.000286 ± 0.000050	0.004950	0.1700 ± 0.0025	10.243 ± 0.156	0.4501 ± 0.0056	0.881	0.1650 ± 0.0012	2396 ± 25	2457 ± 14	2508 ± 12	4.5
8801-10.1	167	80	0.496	85	43	0.000662 ± 0.000185	0.011470	0.1355 ± 0.0084	10.417 ± 0.653	0.4549 ± 0.0135	0.575	0.1661 ± 0.0086	2417 ± 60	2473 ± 60	2519 ± 90	4.0
8801-3.1	191	137	0.739	108	40	0.000502 ± 0.000132	0.008700	0.2081 ± 0.0055	11.038 ± 0.229	0.4763 ± 0.0066	0.750	0.1681 ± 0.0023	2511 ± 29	2526 ± 20	2539 ± 23	1.1
8801-21.1	211	75	0.366	106	42	0.000503 ± 0.000089	0.008720	0.1042 ± 0.0103	10.647 ± 0.342	0.4581 ± 0.0096	0.734	0.1686 ± 0.0037	2431 ± 42	2493 ± 30	2543 ± 37	4.4
8801-17.1	285	131	0.473	153	41	0.000344 ± 0.000043	0.005960	0.1313 ± 0.0028	11.205 ± 0.200	0.4796 ± 0.0061	0.790	0.1694 ± 0.0019	2526 ± 27	2540 ± 17	2552 ± 19	1.0
8801-5.1	491	255	0.537	256	61	0.000312 ± 0.000032	0.005420	0.1473 ± 0.0036	10.779 ± 0.165	0.4605 ± 0.0054	0.836	0.1698 ± 0.0014	2442 ± 24	2504 ± 14	2556 ± 14	4.5
8801-19.1	215	99	0.476	111	37	0.000437 ± 0.000066	0.007570	0.1271 ± 0.0046	10.815 ± 0.372	0.4605 ± 0.0103	0.738	0.1704 ± 0.0040	2442 ± 46	2507 ± 32	2561 ± 40	4.7
8801-4.1	277	243	0.907	160	47	0.000424 ± 0.000055	0.007350	0.2591 ± 0.0031	11.045 ± 0.169	0.4676 ± 0.0058	0.870	0.1713 ± 0.0013	2473 ± 25	2527 ± 14	2571 ± 13	3.8
8801-2.2	175	70	0.410	91	57	0.000793 ± 0.000197	0.013750	0.1116 ± 0.0078	11.198 ± 0.319	0.4701 ± 0.0070	0.624	0.1728 ± 0.0039	2484 ± 31	2540 ± 27	2585 ± 38	3.9
8801-16.1	97	135	1.437	63	32	0.000816 ± 0.000113	0.014140	0.4442 ± 0.0133	11.426 ± 0.523	0.4649 ± 0.0124	0.673	0.1783 ± 0.0061	2461 ± 55	2559 ± 44	2637 ± 58	6.7
8801-8.1	212	129	0.627	116	40	0.000458 ± 0.000066	0.007940	0.1672 ± 0.0044	11.316 ± 0.217	0.4750 ± 0.0061	0.756	0.1728 ± 0.0022	2505 ± 27	2550 ± 18	2585 ± 21	3.1
8801-15.1	216	120	0.577	140	33	0.000323 ± 0.000110	0.005590	0.1582 ± 0.0047	16.050 ± 0.378	0.5512 ± 0.0097	0.822	0.2112 ± 0.0029	2830 ± 41	2880 ± 23	2915 ± 22	2.9
c) Sample 05RAYAH194A2 - Sillimanite-biotite psammitic schist from the Northern Chantrey group. UTM: 554880E, 7643232N																
8802-15.4	421	155	0.381	162	141	0.001077 ± 0.000164	0.018670	0.1040 ± 0.0065	7.683 ± 0.212	0.3557 ± 0.0061	0.711	0.1567 ± 0.0031	1962 ± 29	2195 ± 25	2420 ± 34	18.9
8802-15.2	270	92	0.352	127	204	0.001952 ± 0.000101	0.033820	0.0928 ± 0.0046	9.530 ± 0.193	0.4357 ± 0.0060	0.761	0.1586 ± 0.0021	2331 ± 27	2390 ± 19	2441 ± 23	4.5
8802-15.1	268	93	0.358	133	26	0.000249 ± 0.000030	0.004320	0.1001 ± 0.0015	10.095 ± 0.139	0.4580 ± 0.0055	0.925	0.1599 ± 0.0008	2431 ± 24	2444 ± 13	2454 ± 9	1.0
8802-15.1.2	267	91	0.353	129	13	0.000125 ± 0.000042	0.002160	0.1027 ± 0.0030	9.820 ± 0.256	0.4432 ± 0.0104	0.938	0.1607 ± 0.0015	2365 ± 46	2418 ± 24	2463 ± 16	4.0
8802-15.3	325	119	0.377	150	36	0.000303 ± 0.000052	0.005240	0.1020 ± 0.0037	9.436 ± 0.180	0.4246 ± 0.0065	0.870	0.1612 ± 0.0015	2281 ± 30	2381 ± 18	2468 ± 16	7.6
8802-31.1	54	27	0.514	28	20	0.000914 ± 0.000154	0.015840	0.1518 ± 0.0094	10.190 ± 0.295	0.4557 ± 0.0090	0.760	0.1622 ± 0.0031	2420 ± 40	2452 ± 27	2479 ± 32	2.3
8802-124.1	441	165	0.387	223	29	0.000163 ± 0.000037	0.002830	0.1103 ± 0.0018	10.392 ± 0.142	0.4605 ± 0.0052	0.882	0.1637 ± 0.0011	2442 ± 23	2470 ± 13	2494 ± 11	2.1
8802-11.1	201	103	0.527	106	14	0.000172 ± 0.000033	0.002980	0.1472 ± 0.0020	10.600 ± 0.152	0.4677 ± 0.0055	0.875	0.1644 ± 0.0012	2473 ± 24	2489 ± 13	2501 ± 12	1.1

[a] Spot name follows the convention x-y.z; where x = sample number, y = grain number, and z = spot number. Multiple analyses in an individual spot are labelled as x-y.z.z

[b] Uncertainties reported at 1s (absolute) and are calculated by numerical propagation of all known sources of error.

[c] f206^{204} refers to mole fraction of total ^{206}Pb that is due to common Pb, calculated using the ^{204}Pb-method; common Pb composition used is the surface blank (4/6: 0.05770; 7/6: 0.89500; 8/6: 2.13840).

[d] Corr Coeff = correlation coefficient;

[e] Discordance relative to origin = 100 * (1-(^{206}Pb/^{238}U age)/(^{207}Pb/^{206}Pb age))

*refers to radiogenic Pb (corrected for common Pb)

Calibration standard 6266; U = 910 ppm; age = 559 Ma; ^{206}Pb/^{238}U = 0.09059; error in ^{206}Pb/^{238}U calibration = 1.0%

Grains with multiple analyses in the same location have increased discordance to less than 19%.

APPENDIX A (cont.)

Spot[a]	U (ppm)	Th (ppm)	Th/U	Pb* (ppm)	^{204}Pb (ppb)	^{204}Pb/^{206}Pb	f(206)^{204} [c]	^{208*}Pb/^{206*}Pb	^{207*}Pb/^{235}U	^{206*}Pb/^{238}U	Corr Coeff[d]	^{207*}Pb/^{206*}Pb	Apparent ages (Ma)[b] ^{206}Pb/^{238}U	^{207}Pb/^{235}U	^{207}Pb/^{206}Pb	Disc. (%)[e]
8802-10.1	325	174	0.552	174	11	0.000086 ± 0.000018	0.001490	0.1566 ± 0.0015	10.696 ± 0.141	0.4698 ± 0.0053	0.910	0.1651 ± 0.0009	2483 ± 23	2497 ± 12	2509 ± 9	1.0
8802-76.1	312	163	0.540	159	44	0.000364 ± 0.000045	0.006310	0.1530 ± 0.0040	10.307 ± 0.195	0.4501 ± 0.0069	0.876	0.1661 ± 0.0015	2396 ± 31	2463 ± 18	2519 ± 16	4.9
8802-37.1	172	61	0.369	88	25	0.000356 ± 0.000100	0.006160	0.1023 ± 0.0040	10.818 ± 0.198	0.4673 ± 0.0059	0.768	0.1679 ± 0.0020	2472 ± 26	2508 ± 17	2537 ± 20	2.6
8802-139.1	472	216	0.474	254	23	0.000117 ± 0.000025	0.002020	0.1307 ± 0.0015	11.240 ± 0.143	0.4810 ± 0.0055	0.936	0.1695 ± 0.0008	2532 ± 24	2543 ± 12	2553 ± 8	0.8
8802-111.1	180	64	0.368	92	17	0.000233 ± 0.000058	0.004040	0.1027 ± 0.0029	10.898 ± 0.208	0.4655 ± 0.0066	0.815	0.1698 ± 0.0019	2464 ± 29	2514 ± 18	2556 ± 19	3.6
8802-126.1	345	127	0.382	182	28	0.000200 ± 0.000040	0.003470	0.1063 ± 0.0035	11.306 ± 0.160	0.4802 ± 0.0059	0.912	0.1708 ± 0.0010	2528 ± 26	2549 ± 13	2565 ± 10	1.4
8802-18.1	363	84	0.240	185	19	0.000129 ± 0.000020	0.002240	0.0654 ± 0.0010	11.308 ± 0.139	0.4797 ± 0.0053	0.946	0.1710 ± 0.0007	2526 ± 23	2549 ± 12	2567 ± 7	1.6
8802-61.1	120	48	0.416	64	40	0.000804 ± 0.000099	0.013930	0.1189 ± 0.0050	11.270 ± 0.257	0.4766 ± 0.0085	0.849	0.1715 ± 0.0021	2512 ± 37	2546 ± 21	2572 ± 20	2.3
8802-138.1	341	106	0.322	179	47	0.000332 ± 0.000065	0.005750	0.0875 ± 0.0033	11.446 ± 0.179	0.4839 ± 0.0060	0.852	0.1715 ± 0.0014	2544 ± 26	2560 ± 15	2573 ± 14	1.1
8802-92.1	240	236	1.018	143	32	0.000321 ± 0.000093	0.005560	0.2814 ± 0.0108	11.314 ± 0.615	0.4769 ± 0.0171	0.745	0.1721 ± 0.0063	2514 ± 75	2549 ± 52	2578 ± 62	2.5
8802-6.1	224	90	0.416	120	16	0.000175 ± 0.000053	0.003030	0.1147 ± 0.0024	11.418 ± 0.172	0.4810 ± 0.0056	0.839	0.1722 ± 0.0014	2532 ± 24	2558 ± 14	2579 ± 14	1.8
8802-95.1	297	99	0.345	159	44	0.000350 ± 0.000052	0.006060	0.0997 ± 0.0031	11.577 ± 0.213	0.4876 ± 0.0067	0.822	0.1722 ± 0.0018	2560 ± 29	2571 ± 17	2579 ± 18	0.7
8802-87.1	207	82	0.409	111	48	0.000555 ± 0.000075	0.009610	0.1098 ± 0.0034	11.536 ± 0.534	0.4855 ± 0.0072	0.432	0.1723 ± 0.0073	2551 ± 31	2567 ± 44	2580 ± 72	1.1
8802-68.1	188	85	0.466	105	44	0.000547 ± 0.000085	0.009470	0.1309 ± 0.0049	11.758 ± 0.261	0.4944 ± 0.0083	0.831	0.1725 ± 0.0021	2590 ± 36	2585 ± 21	2582 ± 21	0.3
8802-141.1	315	235	0.771	181	37	0.000281 ± 0.000041	0.004870	0.2127 ± 0.0030	11.445 ± 0.215	0.4811 ± 0.0070	0.841	0.1726 ± 0.0018	2532 ± 31	2560 ± 18	2583 ± 17	2.0
8802-82.1	274	93	0.350	146	42	0.000366 ± 0.000085	0.006350	0.0939 ± 0.0035	11.603 ± 0.211	0.4877 ± 0.0068	0.837	0.1726 ± 0.0017	2561 ± 30	2573 ± 17	2583 ± 17	0.8
8802-69.1	228	156	0.704	129	34	0.000361 ± 0.000061	0.006260	0.2027 ± 0.0034	11.365 ± 0.176	0.4776 ± 0.0054	0.802	0.1726 ± 0.0016	2517 ± 24	2554 ± 15	2583 ± 16	2.5
8802-42.1	302	106	0.361	161	17	0.000132 ± 0.000021	0.002290	0.1039 ± 0.0018	11.524 ± 0.141	0.4843 ± 0.0052	0.929	0.1726 ± 0.0008	2546 ± 23	2567 ± 12	2583 ± 8	1.4
8802-93.1	302	150	0.512	165	28	0.000222 ± 0.000078	0.003850	0.1447 ± 0.0046	11.458 ± 0.224	0.4810 ± 0.0070	0.814	0.1728 ± 0.0020	2532 ± 30	2561 ± 18	2585 ± 19	2.0
8802-88.1	233	70	0.311	122	42	0.000429 ± 0.000116	0.007440	0.0869 ± 0.0050	11.525 ± 0.244	0.4831 ± 0.0066	0.731	0.1730 ± 0.0025	2541 ± 29	2567 ± 20	2587 ± 24	1.8
8802-135.1	295	121	0.424	159	52	0.000420 ± 0.000047	0.007270	0.1161 ± 0.0024	11.599 ± 0.372	0.4853 ± 0.0065	0.524	0.1733 ± 0.0048	2550 ± 28	2573 ± 30	2590 ± 47	1.5
8802-41.1	157	52	0.339	82	20	0.000311 ± 0.000042	0.005390	0.0911 ± 0.0025	11.522 ± 0.202	0.4820 ± 0.0064	0.826	0.1734 ± 0.0017	2536 ± 28	2566 ± 17	2591 ± 17	2.1
8802-104.1	310	189	0.629	173	11	0.000088 ± 0.000038	0.001520	0.1786 ± 0.0024	11.501 ± 0.207	0.4794 ± 0.0064	0.819	0.1740 ± 0.0018	2525 ± 28	2565 ± 17	2596 ± 17	2.8
8802-119.1	253	126	0.514	141	26	0.000244 ± 0.000044	0.004230	0.1411 ± 0.0039	11.800 ± 0.161	0.4905 ± 0.0055	0.877	0.1745 ± 0.0012	2573 ± 24	2589 ± 13	2601 ± 11	1.1
8802-50.1	356	106	0.307	185	21	0.000140 ± 0.000038	0.002430	0.0875 ± 0.0024	11.547 ± 0.155	0.4794 ± 0.0054	0.902	0.1747 ± 0.0010	2525 ± 24	2568 ± 13	2603 ± 10	3.0
8802-120.1	246	126	0.526	135	47	0.000458 ± 0.000061	0.007930	0.1426 ± 0.0039	11.630 ± 0.170	0.4827 ± 0.0056	0.859	0.1747 ± 0.0013	2539 ± 24	2575 ± 14	2604 ± 13	2.5
8802-79.1	326	210	0.665	184	49	0.000359 ± 0.000104	0.006220	0.1796 ± 0.0045	11.645 ± 0.240	0.4831 ± 0.0059	0.684	0.1748 ± 0.0027	2541 ± 26	2576 ± 19	2604 ± 25	2.4
8802-28.1	160	185	1.195	101	13	0.000193 ± 0.000033	0.003350	0.3315 ± 0.0028	11.785 ± 0.185	0.4879 ± 0.0057	0.813	0.1752 ± 0.0016	2562 ± 25	2587 ± 15	2608 ± 15	1.8
8802-97.1	136	74	0.562	75	41	0.000722 ± 0.000094	0.012510	0.1592 ± 0.0049	11.596 ± 0.318	0.4798 ± 0.0077	0.676	0.1753 ± 0.0036	2526 ± 34	2572 ± 26	2609 ± 34	3.2
8802-13.1	227	209	0.951	138	12	0.000123 ± 0.000026	0.002140	0.2578 ± 0.0026	11.916 ± 0.178	0.4910 ± 0.0061	0.887	0.1760 ± 0.0012	2575 ± 26	2598 ± 14	2616 ± 12	1.5
8802-12.1	193	171	0.914	117	13	0.000155 ± 0.000039	0.002680	0.2585 ± 0.0047	11.941 ± 0.156	0.4913 ± 0.0055	0.915	0.1763 ± 0.0009	2576 ± 24	2600 ± 12	2618 ± 9	1.6
8802-60.1	98	63	0.664	55	49	0.001197 ± 0.000149	0.020740	0.1907 ± 0.0067	11.638 ± 0.278	0.4788 ± 0.0069	0.695	0.1763 ± 0.0031	2522 ± 30	2576 ± 23	2618 ± 29	3.7
8802-78.1	391	115	0.303	205	31	0.000190 ± 0.000029	0.003290	0.0884 ± 0.0029	11.746 ± 0.188	0.4817 ± 0.0062	0.864	0.1768 ± 0.0014	2535 ± 27	2584 ± 15	2623 ± 14	3.4
8802-70.1	314	176	0.580	178	22	0.000165 ± 0.000034	0.002850	0.1679 ± 0.0038	12.000 ± 0.184	0.4886 ± 0.0056	0.821	0.1781 ± 0.0016	2565 ± 24	2604 ± 14	2636 ± 15	2.7
8802-8.1	276	198	0.741	165	16	0.000136 ± 0.000036	0.002370	0.2031 ± 0.0023	12.422 ± 0.172	0.5028 ± 0.0063	0.942	0.1792 ± 0.0008	2626 ± 27	2637 ± 13	2645 ± 8	0.7
8802-40.1	273	72	0.272	150	15	0.000129 ± 0.000027	0.002240	0.0768 ± 0.0014	12.602 ± 0.157	0.5100 ± 0.0056	0.931	0.1792 ± 0.0008	2656 ± 24	2650 ± 12	2646 ± 8	0.4
8802-143.1	115	52	0.466	63	30	0.000631 ± 0.000157	0.010930	0.1430 ± 0.0065	11.945 ± 0.282	0.4815 ± 0.0074	0.737	0.1799 ± 0.0029	2534 ± 32	2600 ± 22	2652 ± 27	4.5
8802-96.1	100	63	0.657	59	42	0.000954 ± 0.000120	0.016540	0.1753 ± 0.0066	12.666 ± 0.257	0.5094 ± 0.0067	0.729	0.1804 ± 0.0025	2654 ± 28	2655 ± 19	2656 ± 23	0.1
8802-52.1	131	102	0.803	78	15	0.000273 ± 0.000073	0.004730	0.2332 ± 0.0038	12.115 ± 0.214	0.4867 ± 0.0064	0.812	0.1805 ± 0.0019	2556 ± 28	2613 ± 17	2658 ± 17	3.8
8802-130.1	236	104	0.454	135	38	0.000372 ± 0.000095	0.006440	0.1253 ± 0.0040	12.718 ± 0.243	0.5080 ± 0.0065	0.750	0.1816 ± 0.0023	2648 ± 28	2659 ± 18	2667 ± 21	0.7
8802-142.1	357	108	0.312	191	35	0.000235 ± 0.000047	0.004070	0.0846 ± 0.0024	12.321 ± 0.315	0.4906 ± 0.0093	0.810	0.1821 ± 0.0028	2573 ± 40	2629 ± 24	2672 ± 25	3.7
8802-9.1	107	47	0.450	61	20	0.000426 ± 0.000116	0.007380	0.1201 ± 0.0055	12.716 ± 0.220	0.5058 ± 0.0059	0.754	0.1823 ± 0.0021	2639 ± 25	2659 ± 16	2674 ± 19	1.3
8802-65.1	246	307	1.289	164	38	0.000355 ± 0.000057	0.006160	0.3532 ± 0.0034	12.666 ± 0.327	0.5036 ± 0.0058	0.552	0.1824 ± 0.0040	2629 ± 25	2655 ± 25	2675 ± 36	1.7
8802-85.1	215	87	0.418	123	35	0.000372 ± 0.000061	0.006450	0.1151 ± 0.0028	12.893 ± 0.218	0.5109 ± 0.0067	0.838	0.1830 ± 0.0017	2660 ± 28	2672 ± 16	2681 ± 15	0.8
8802-100.1	70	43	0.634	40	46	0.001534 ± 0.000322	0.026590	0.1788 ± 0.0148	12.324 ± 0.510	0.4862 ± 0.0088	0.541	0.1839 ± 0.0065	2554 ± 38	2629 ± 40	2688 ± 59	5.0
8802-29.1	298	96	0.335	167	27	0.000206 ± 0.000024	0.003580	0.0905 ± 0.0014	13.059 ± 0.158	0.5126 ± 0.0056	0.942	0.1848 ± 0.0008	2668 ± 24	2684 ± 11	2696 ± 7	1.1
8802-39.1	164	79	0.499	96	15	0.000209 ± 0.000035	0.003610	0.1413 ± 0.0022	13.222 ± 0.219	0.5158 ± 0.0063	0.816	0.1859 ± 0.0018	2681 ± 27	2696 ± 16	2706 ± 16	0.9
8802-7.1	141	49	0.361	80	18	0.000290 ± 0.000056	0.005020	0.1008 ± 0.0032	13.124 ± 0.189	0.5120 ± 0.0060	0.880	0.1859 ± 0.0013	2665 ± 26	2689 ± 14	2706 ± 11	1.5
8802-136.1	143	78	0.562	82	44	0.000702 ± 0.000174	0.012160	0.1433 ± 0.0090	12.969 ± 0.312	0.5050 ± 0.0069	0.660	0.1863 ± 0.0034	2635 ± 30	2677 ± 23	2709 ± 30	2.7

APPENDIX A (cont.)

Spot[a]	U (ppm)	Th (ppm)	Th/U	Pb* (ppm)	^{204}Pb (ppb)	^{204}Pb/^{206}Pb	f(206)^{204} [c]	^{208*}Pb/^{206*}Pb	^{207*}Pb/^{235}U	^{206*}Pb/^{238}U	Corr Coeff[d]	^{207*}Pb/^{206*}Pb	Apparent ages (Ma)[b] ^{206}Pb/^{238}U	^{207}Pb/^{235}U	^{207}Pb/^{206}Pb	Disc. (%)[e]
8802-128.1	222	89	0.414	128	34	0.000348 ± 0.000052	0.006030	0.1185 ± 0.0034	13.184 ± 0.233	0.5127 ± 0.0075	0.884	0.1865 ± 0.0016	2668 ± 32	2693 ± 17	2712 ± 14	1.6
8802-22.1	158	116	0.761	98	18	0.000260 ± 0.000082	0.004510	0.2075 ± 0.0040	13.281 ± 0.230	0.5163 ± 0.0066	0.809	0.1865 ± 0.0019	2684 ± 28	2700 ± 16	2712 ± 17	1.0
8802-1.1	180	79	0.451	103	28	0.000358 ± 0.000077	0.006210	0.1198 ± 0.0032	13.193 ± 0.193	0.5086 ± 0.0057	0.829	0.1881 ± 0.0016	2650 ± 24	2694 ± 14	2726 ± 14	2.8
8802-36.1	93	135	1.502	67	16	0.000389 ± 0.000065	0.006740	0.4166 ± 0.0060	13.609 ± 0.241	0.5197 ± 0.0072	0.847	0.1899 ± 0.0018	2698 ± 31	2723 ± 17	2742 ± 16	1.6
8802-71.1	286	186	0.672	171	42	0.000336 ± 0.000065	0.005820	0.1837 ± 0.0043	13.279 ± 0.195	0.5061 ± 0.0060	0.869	0.1903 ± 0.0014	2640 ± 26	2700 ± 14	2745 ± 12	3.8
8802-53.1	153	59	0.397	88	17	0.000248 ± 0.000066	0.004310	0.1067 ± 0.0037	13.503 ± 0.234	0.5140 ± 0.0058	0.738	0.1906 ± 0.0023	2674 ± 25	2716 ± 17	2747 ± 20	2.7
8802-145.1	89	50	0.580	50	32	0.000857 ± 0.000126	0.014840	0.1547 ± 0.0119	12.822 ± 0.339	0.4874 ± 0.0086	0.749	0.1908 ± 0.0034	2559 ± 37	2667 ± 25	2749 ± 29	6.9
8802-90.1	52	76	1.508	38	46	0.001882 ± 0.000208	0.032620	0.4143 ± 0.0122	13.917 ± 0.405	0.5284 ± 0.0088	0.666	0.1910 ± 0.0042	2735 ± 37	2744 ± 28	2751 ± 36	0.6
8802-118.1	245	147	0.620	149	50	0.000452 ± 0.000113	0.007840	0.1748 ± 0.0067	13.682 ± 0.264	0.5181 ± 0.0068	0.760	0.1915 ± 0.0024	2691 ± 29	2728 ± 18	2755 ± 21	2.3
8802-147.1	184	100	0.562	110	30	0.000366 ± 0.000066	0.006350	0.1524 ± 0.0033	13.659 ± 0.201	0.5166 ± 0.0059	0.845	0.1917 ± 0.0015	2685 ± 25	2726 ± 14	2757 ± 13	2.6
8802-57.2	112	88	0.813	72	50	0.000961 ± 0.000109	0.016660	0.2205 ± 0.0078	14.048 ± 0.291	0.5283 ± 0.0068	0.712	0.1928 ± 0.0028	2734 ± 29	2753 ± 20	2767 ± 24	1.2
8802-115.1	193	150	0.801	118	45	0.000533 ± 0.000062	0.009240	0.2247 ± 0.0037	13.319 ± 0.258	0.4992 ± 0.0069	0.790	0.1935 ± 0.0023	2610 ± 30	2703 ± 18	2772 ± 20	5.8
8802-116.1	137	26	0.199	76	41	0.000659 ± 0.000119	0.011420	0.0508 ± 0.0061	13.867 ± 0.259	0.5181 ± 0.0062	0.730	0.1941 ± 0.0025	2691 ± 27	2741 ± 18	2777 ± 21	3.1
8802-32.1	55	30	0.566	33	16	0.000661 ± 0.000110	0.011460	0.1649 ± 0.0053	13.912 ± 0.328	0.5197 ± 0.0073	0.686	0.1942 ± 0.0034	2698 ± 31	2744 ± 23	2778 ± 29	2.9
8802-72.1	45	45	1.031	29	28	0.001427 ± 0.000270	0.024740	0.2923 ± 0.0126	13.523 ± 0.470	0.5050 ± 0.0078	0.547	0.1942 ± 0.0057	2635 ± 33	2717 ± 33	2778 ± 49	5.2
8802-102.1	80	108	1.399	57	30	0.000849 ± 0.000161	0.014710	0.4143 ± 0.0131	13.900 ± 0.350	0.5158 ± 0.0078	0.689	0.1955 ± 0.0036	2681 ± 33	2743 ± 24	2789 ± 30	3.9
8802-123.1	157	114	0.748	99	31	0.000440 ± 0.000097	0.007620	0.2047 ± 0.0044	14.081 ± 0.241	0.5217 ± 0.0063	0.784	0.1958 ± 0.0021	2706 ± 27	2755 ± 16	2791 ± 18	3.0
8802-66.1	134	88	0.679	83	49	0.000792 ± 0.000104	0.013730	0.1749 ± 0.0069	14.369 ± 0.362	0.5282 ± 0.0082	0.706	0.1973 ± 0.0036	2734 ± 35	2774 ± 24	2804 ± 30	2.5
8802-17.1	108	39	0.375	64	21	0.000425 ± 0.000062	0.007360	0.1004 ± 0.0028	14.511 ± 0.240	0.5324 ± 0.0063	0.790	0.1977 ± 0.0020	2752 ± 26	2784 ± 16	2807 ± 17	2.0
8802-67.1	58	67	1.197	41	39	0.001455 ± 0.000326	0.025220	0.3374 ± 0.0136	14.533 ± 0.492	0.5321 ± 0.0081	0.552	0.1981 ± 0.0056	2750 ± 34	2785 ± 33	2811 ± 47	2.1
8802-105.1	350	445	1.313	251	41	0.000258 ± 0.000033	0.004470	0.3775 ± 0.0029	14.402 ± 0.193	0.5272 ± 0.0062	0.924	0.1981 ± 0.0010	2730 ± 26	2777 ± 13	2811 ± 8	2.9
8802-64.1	119	89	0.774	78	42	0.000749 ± 0.000094	0.012990	0.2103 ± 0.0046	14.787 ± 0.273	0.5398 ± 0.0067	0.758	0.1987 ± 0.0024	2782 ± 28	2802 ± 18	2815 ± 20	1.2
8802-34.1	158	231	1.514	117	18	0.000255 ± 0.000039	0.004420	0.4194 ± 0.0036	14.698 ± 0.215	0.5319 ± 0.0064	0.878	0.2004 ± 0.0014	2750 ± 27	2796 ± 14	2829 ± 12	2.8
8802-83.1	104	74	0.735	67	74	0.001505 ± 0.000170	0.026090	0.2001 ± 0.0097	14.870 ± 0.371	0.5354 ± 0.0088	0.745	0.2014 ± 0.0034	2764 ± 37	2807 ± 24	2838 ± 28	2.6
8802-106.1	161	51	0.328	94	25	0.000347 ± 0.000184	0.006010	0.0868 ± 0.0072	14.743 ± 0.365	0.5284 ± 0.0089	0.764	0.2024 ± 0.0033	2735 ± 38	2799 ± 24	2845 ± 26	3.9
8802-110.1	151	54	0.365	91	6	0.000091 ± 0.000040	0.001580	0.0948 ± 0.0029	15.151 ± 0.336	0.5401 ± 0.0080	0.747	0.2035 ± 0.0030	2784 ± 33	2825 ± 21	2854 ± 24	2.5
8802-27.1	52	40	0.786	34	17	0.000677 ± 0.000110	0.011730	0.2104 ± 0.0057	15.298 ± 0.375	0.5425 ± 0.0106	0.862	0.2045 ± 0.0026	2794 ± 45	2834 ± 24	2863 ± 21	2.4
8802-117.1	86	52	0.628	55	54	0.001337 ± 0.000151	0.023170	0.1696 ± 0.0078	15.415 ± 0.467	0.5390 ± 0.0090	0.648	0.2074 ± 0.0048	2779 ± 38	2841 ± 29	2886 ± 38	3.7
8802-46.1	91	49	0.552	59	20	0.000457 ± 0.000068	0.007930	0.1528 ± 0.0036	15.940 ± 0.309	0.5566 ± 0.0086	0.857	0.2077 ± 0.0021	2852 ± 36	2873 ± 19	2888 ± 16	1.2
8802-43.1	307	166	0.559	192	35	0.000246 ± 0.000033	0.004260	0.1524 ± 0.0021	15.360 ± 0.224	0.5354 ± 0.0063	0.872	0.2081 ± 0.0015	2764 ± 27	2838 ± 14	2891 ± 12	4.4
8802-20.1	262	139	0.549	169	20	0.000164 ± 0.000028	0.002840	0.1493 ± 0.0030	16.014 ± 0.213	0.5520 ± 0.0064	0.920	0.2104 ± 0.0011	2833 ± 27	2878 ± 13	2909 ± 9	2.6
8802-38.1	43	23	0.539	28	20	0.000965 ± 0.000149	0.016730	0.1430 ± 0.0089	16.469 ± 0.483	0.5627 ± 0.0107	0.732	0.2123 ± 0.0043	2878 ± 44	2904 ± 28	2923 ± 33	1.6
8802-99.1	203	112	0.570	134	43	0.000438 ± 0.000056	0.007580	0.1531 ± 0.0030	16.432 ± 0.305	0.5599 ± 0.0083	0.859	0.2128 ± 0.0020	2866 ± 34	2902 ± 18	2927 ± 16	2.1
8802-132.1	125	66	0.543	87	52	0.000810 ± 0.000172	0.014040	0.1403 ± 0.0069	18.950 ± 0.481	0.5851 ± 0.0116	0.849	0.2349 ± 0.0032	2969 ± 47	3039 ± 25	3086 ± 22	3.8
8802-25.1	37	5	0.126	25	14	0.000697 ± 0.000131	0.012090	0.0360 ± 0.0052	20.166 ± 0.381	0.6049 ± 0.0082	0.797	0.2418 ± 0.0028	3050 ± 33	3099 ± 18	3132 ± 18	2.6
8802-44.1	487	88	0.188	331	37	0.000144 ± 0.000015	0.002500	0.0515 ± 0.0007	20.409 ± 0.250	0.6120 ± 0.0068	0.944	0.2419 ± 0.0010	3078 ± 27	3111 ± 12	3132 ± 6	1.7
8802-5.1	98	58	0.609	76	13	0.000241 ± 0.000048	0.004170	0.1647 ± 0.0041	22.728 ± 0.321	0.6263 ± 0.0077	0.917	0.2632 ± 0.0015	3135 ± 31	3215 ± 14	3266 ± 9	4.0
8802-56.1	23	10	0.432	18	17	0.001305 ± 0.000226	0.022610	0.1210 ± 0.0114	24.684 ± 0.845	0.6531 ± 0.0143	0.725	0.2741 ± 0.0065	3240 ± 56	3296 ± 34	3330 ± 38	2.7
8802-74.1	73	43	0.608	61	55	0.001301 ± 0.000186	0.022550	0.1720 ± 0.0078	26.576 ± 0.668	0.6629 ± 0.0096	0.671	0.2908 ± 0.0055	3278 ± 37	3368 ± 25	3422 ± 30	4.2

[a]Spot name follows the convention x-y.z; where x = sample number, y = grain number and z = spot number. Multiple analyses in an individual spot are labelled as x-y.z.z

[b]Uncertainties reported at 1s (absolute) and are calculated by numerical propagation of all known sources of error.

[c]f206^{204} refers to mole fraction of total ^{206}Pb that is due to common Pb, calculated using the ^{204}Pb-method; common Pb composition used is the surface blank (4/6: 0.05770; 7/6: 0.89500; 8/6: 2.13840).

[d]Corr Coeff = correlation coefficient

[e]Discordance relative to origin = 100 * (1-(^{206}Pb/^{238}U age)/(^{207}Pb/^{206}Pb age))

*refers to radiogenic Pb (corrected for common Pb)

Calibration standard 6266; U = 910 ppm; age = 559 Ma; ^{206}Pb/^{238}U = 0.09059; error in ^{206}Pb/^{238}U calibration = 1.0%

Grains with multiple analyses in the same location have increased discordance to less than 19%.